

An investigation of the screen grid tap

A search for the hidden arguments.

By Rudolf Moers

APPENDICES

Mentioned screen grid taps x_{TURNS} in these appendices are the values from column 3 of table 7.

For all anode characteristics in appendix A, C and E, the V_{gIk} -curves in the intervals $0V \leq V_{ak} \leq 300V$ are measured with the μ Tracer and the V_{gIk} -curves in the intervals $300V \leq V_{ak} \leq 600V$ are extrapolated, so not measured.

By this 5 or 4 points of intersection on the load line are made with measured V_{gIk} -curves and the other 3 or 4 points of intersection on the load line are made with extrapolated V_{gIk} -curves.

- A. Measured with the μ Tracer and extrapolated anode characteristics of EL84 for several screen grid taps. Load line for EL84 goes through working point $V_{ak,w} = 300V$, $I_{a,w} = 40mA$ and $V_{gIk,w} \approx -9.1V$.
- B. Constructed dynamic transconductance characteristics of EL84 for several screen grid taps.
- C. Measured with the μ Tracer and extrapolated anode characteristics of EL34 for several screen grid taps. Load line for EL34 goes through working point $V_{ak,w} = 300V$, $I_{a,w} = 80mA$ and $V_{gIk,w} \approx -16.1V$.
- D. Constructed dynamic transconductance characteristics of EL34 for several screen grid taps.
- E. Measured with the μ Tracer and extrapolated anode characteristics of KT88 for several screen grid taps. Load line for KT88 goes through working point $V_{ak,w} = 300V$, $I_{a,w} = 80mA$ and $V_{gIk,w} \approx -26.4V$.
- F. Constructed dynamic transconductance characteristics of KT88 for several screen grid taps.

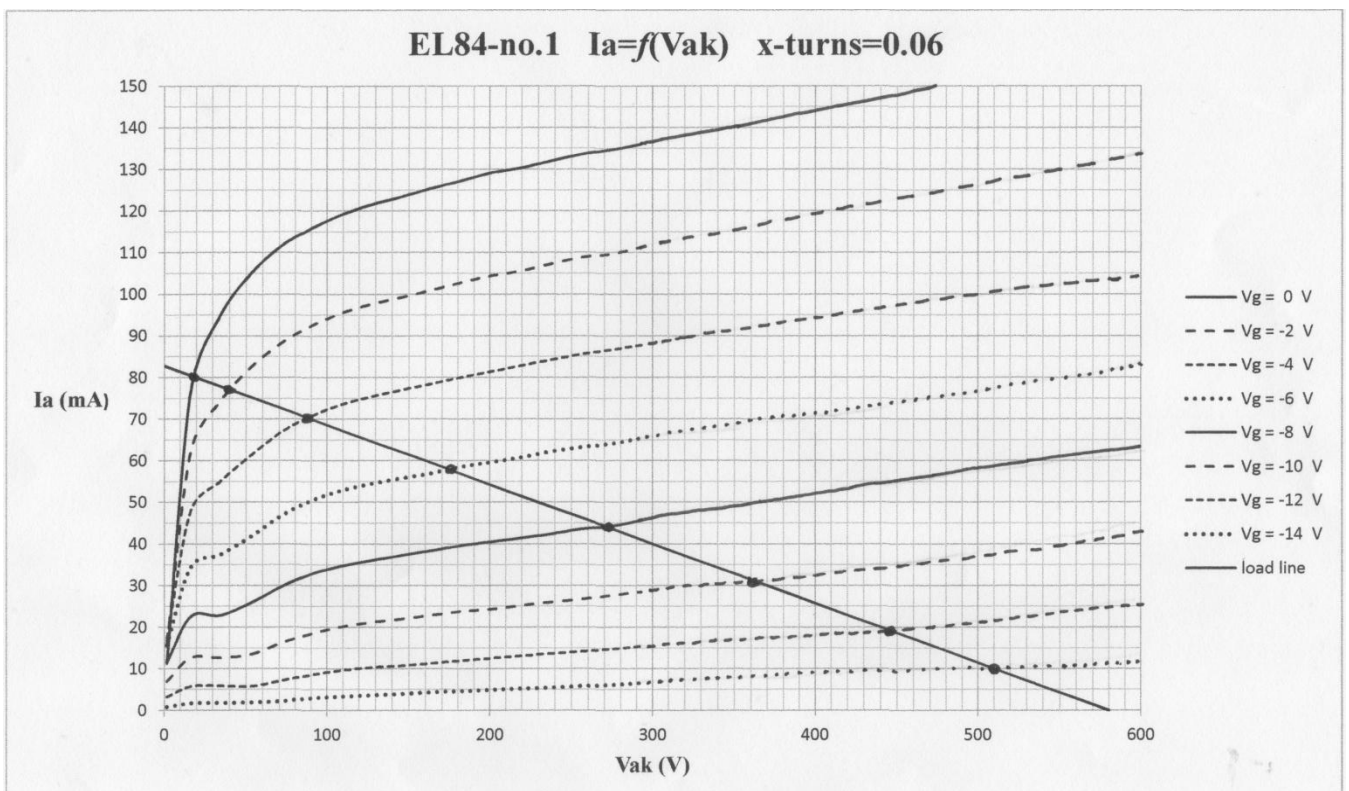
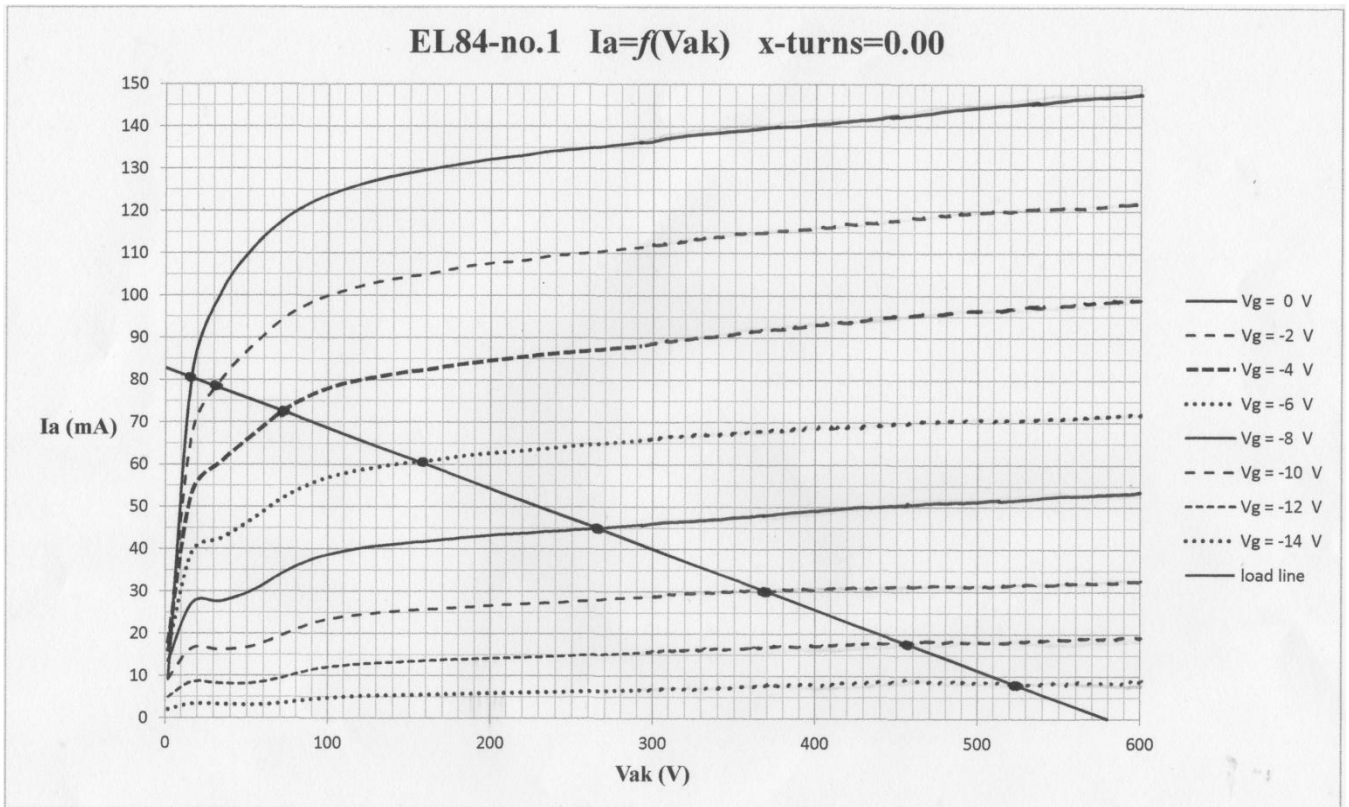
The constructed dynamic transconductances of appendix B are derived from the anode characteristics of appendix A (see the points of intersection of the V_{gIk} -curves with the load lines).

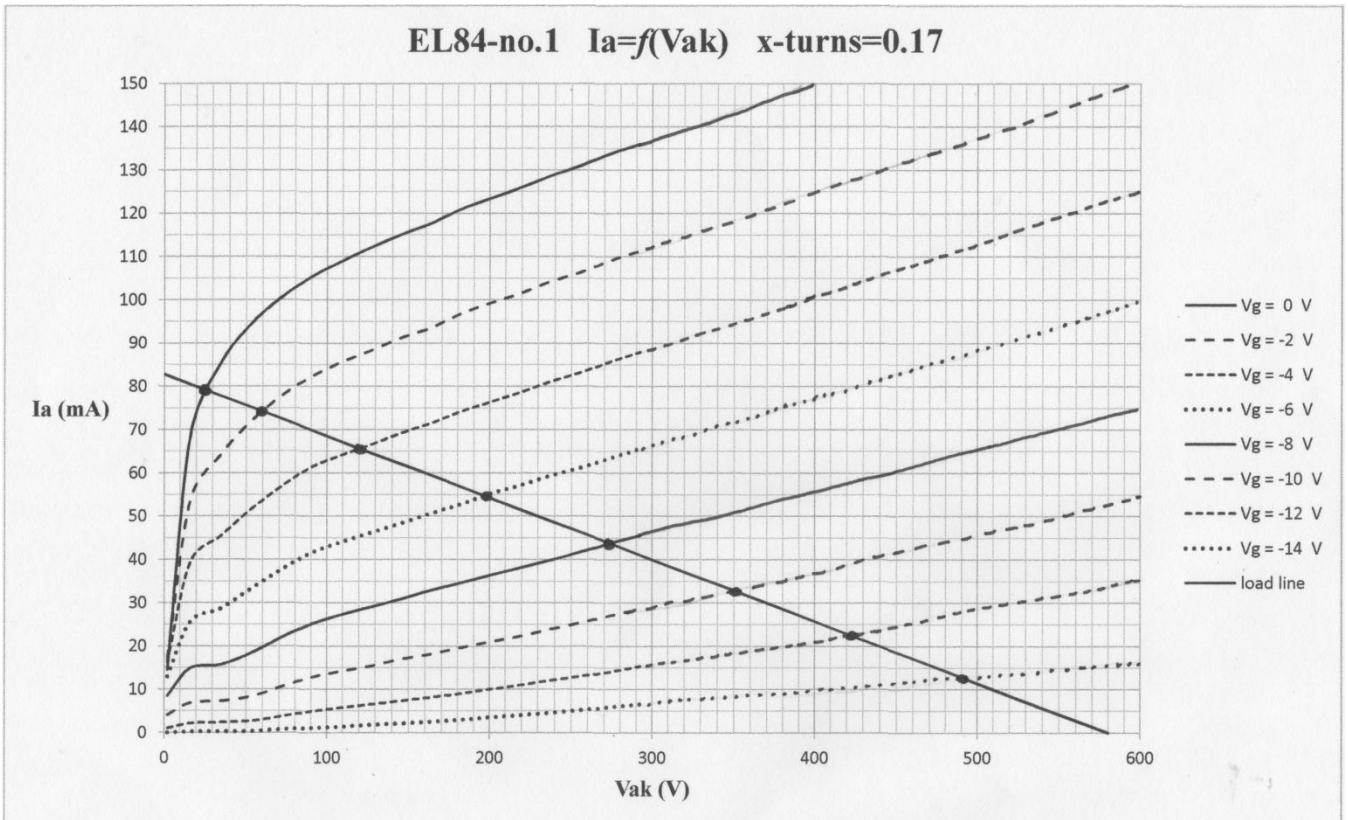
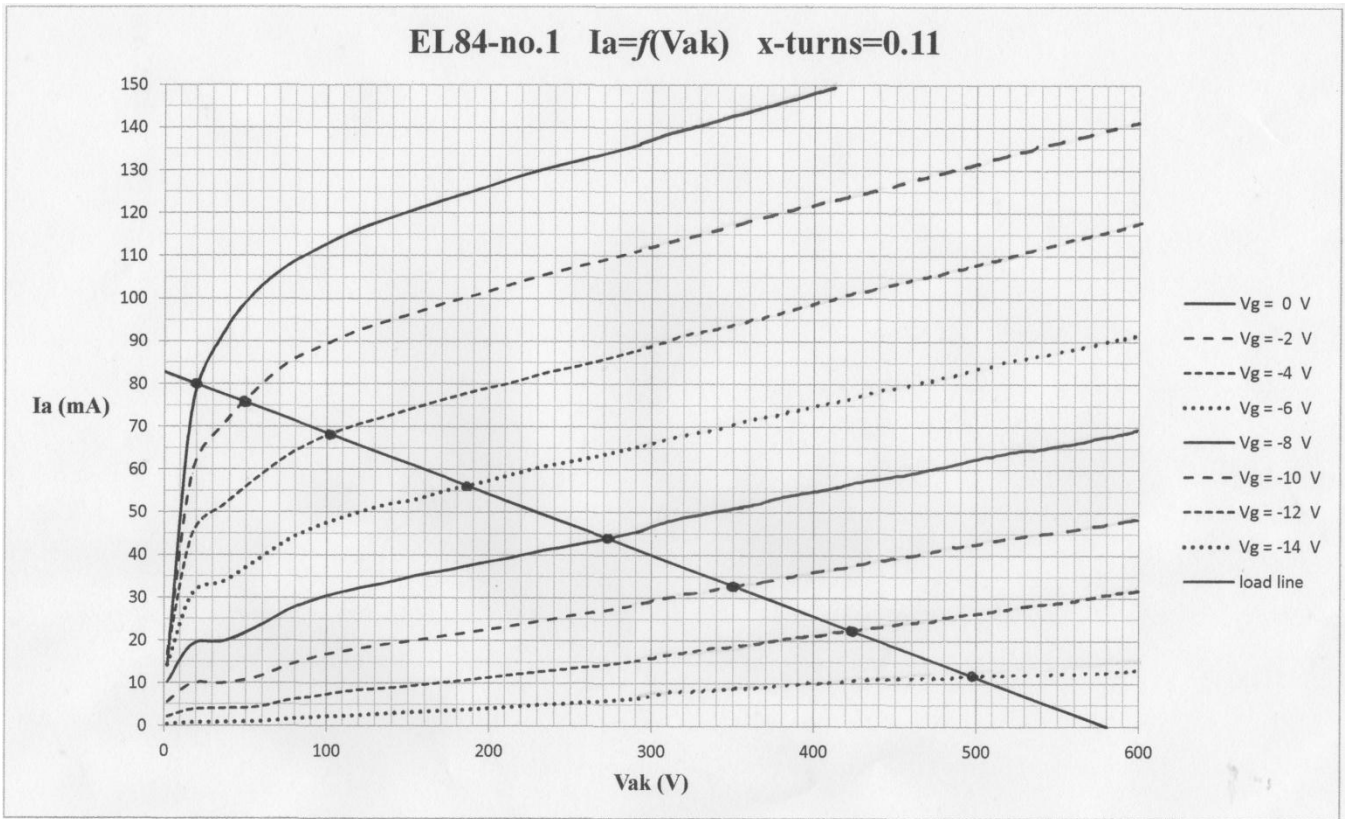
The constructed dynamic transconductances of appendix D are derived from the anode characteristics of appendix C (see the points of intersection of the V_{gIk} -curves with the load lines).

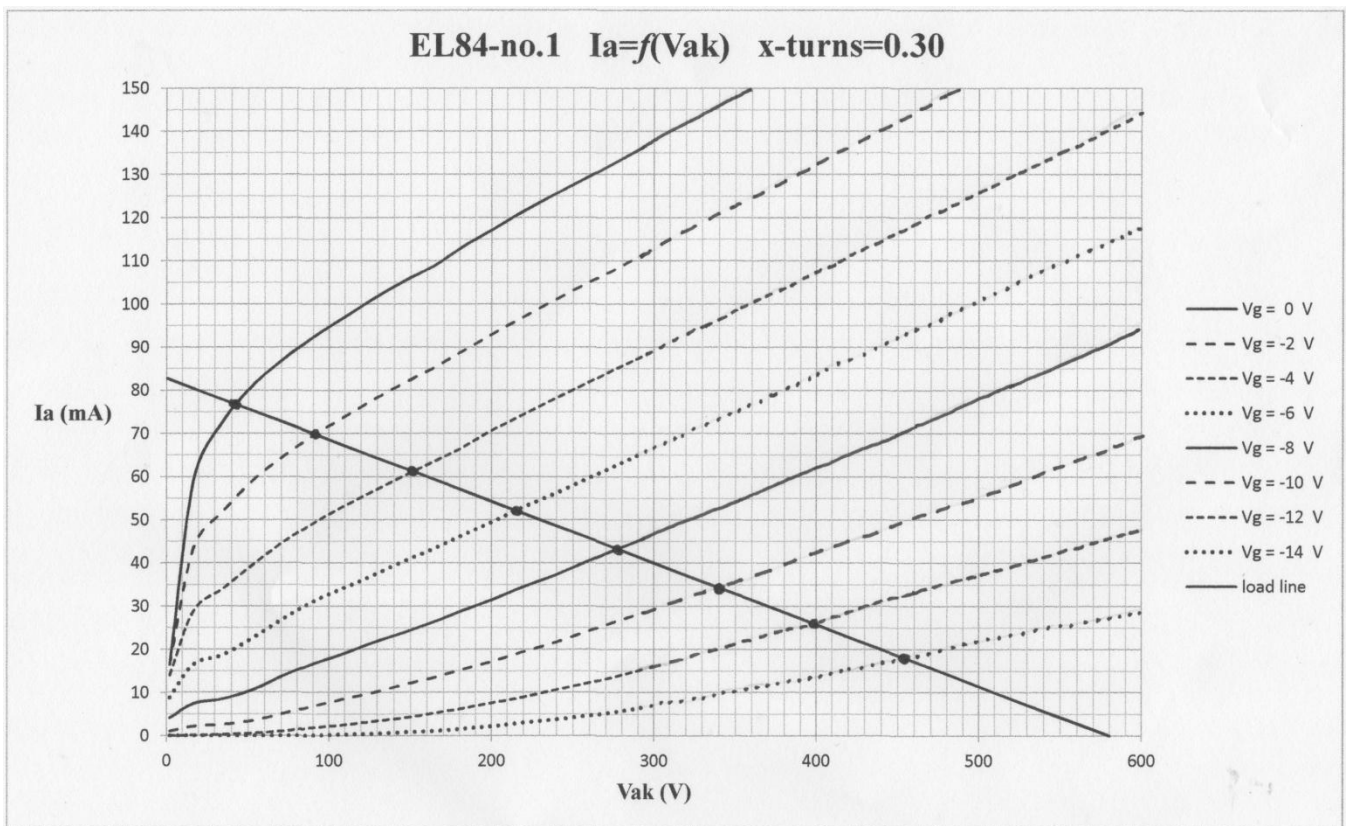
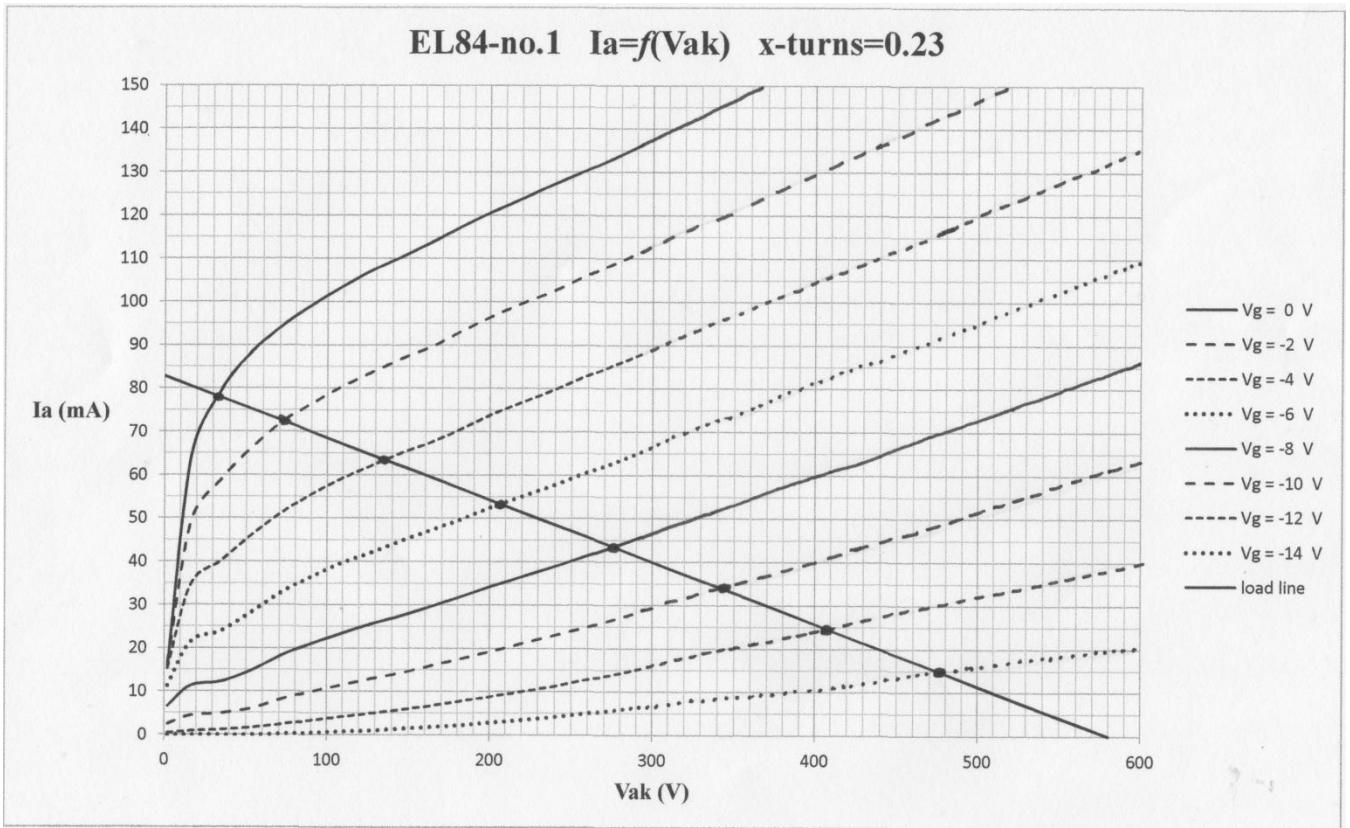
The constructed dynamic transconductances of appendix F are derived from the anode characteristics of appendix E (see the points of intersection of the V_{gIk} -curves with the load lines).

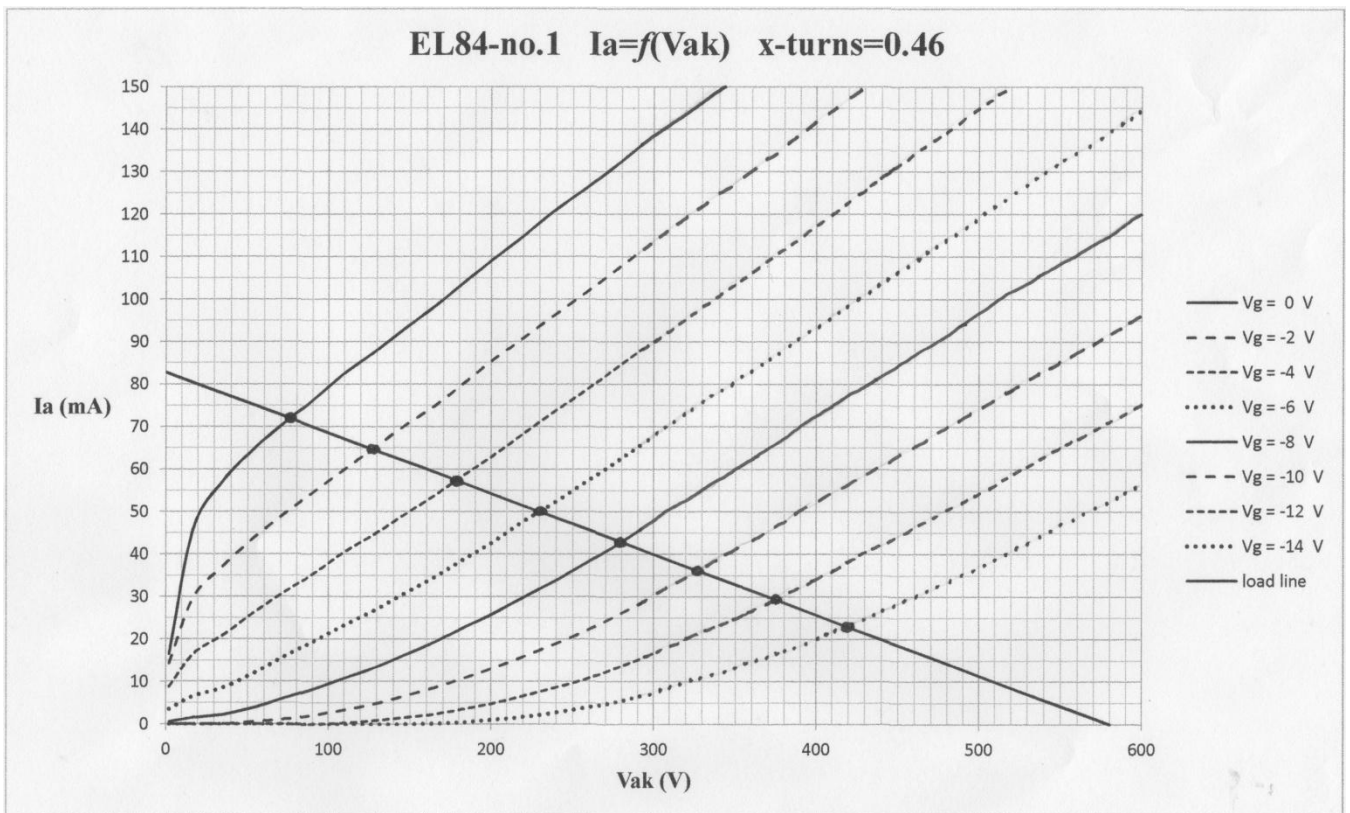
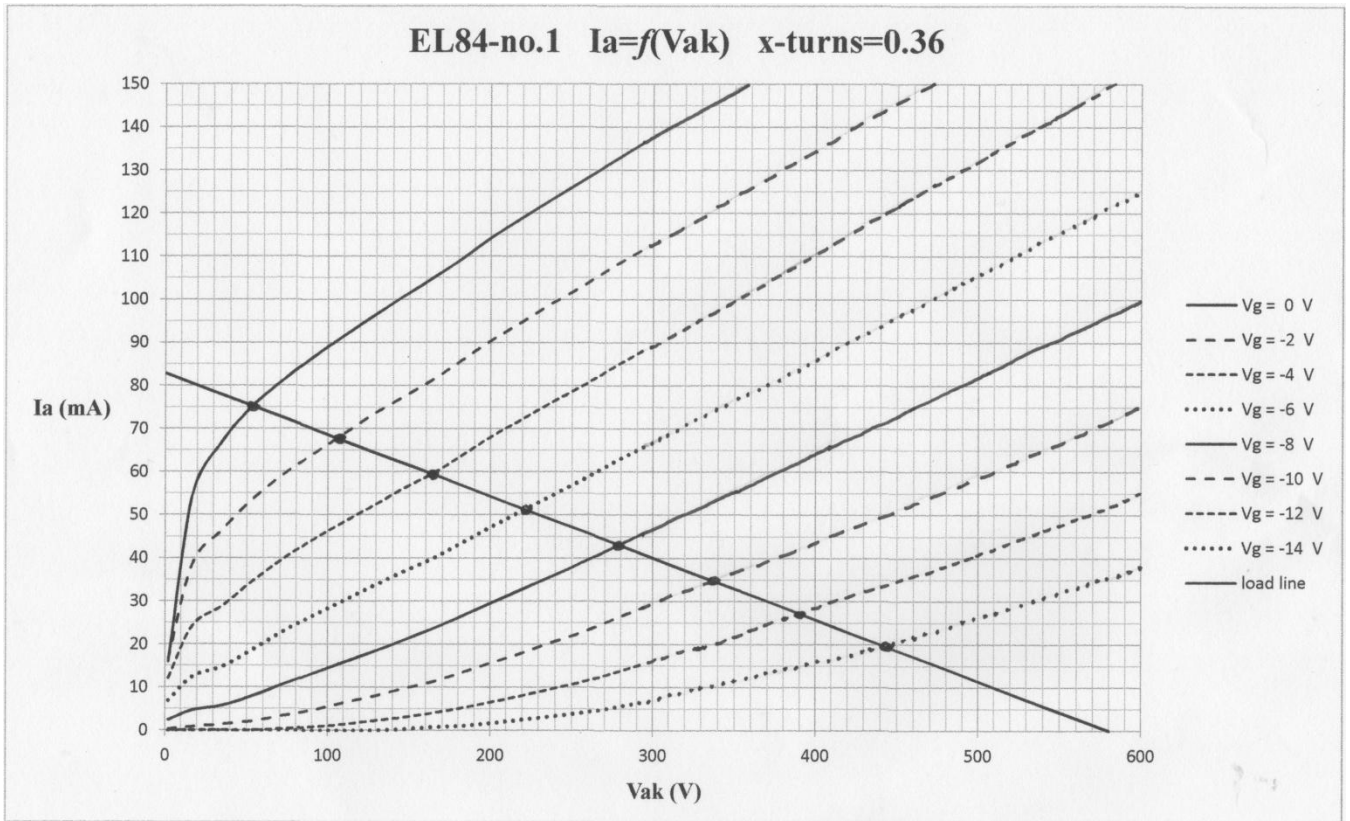
APPENDIX A

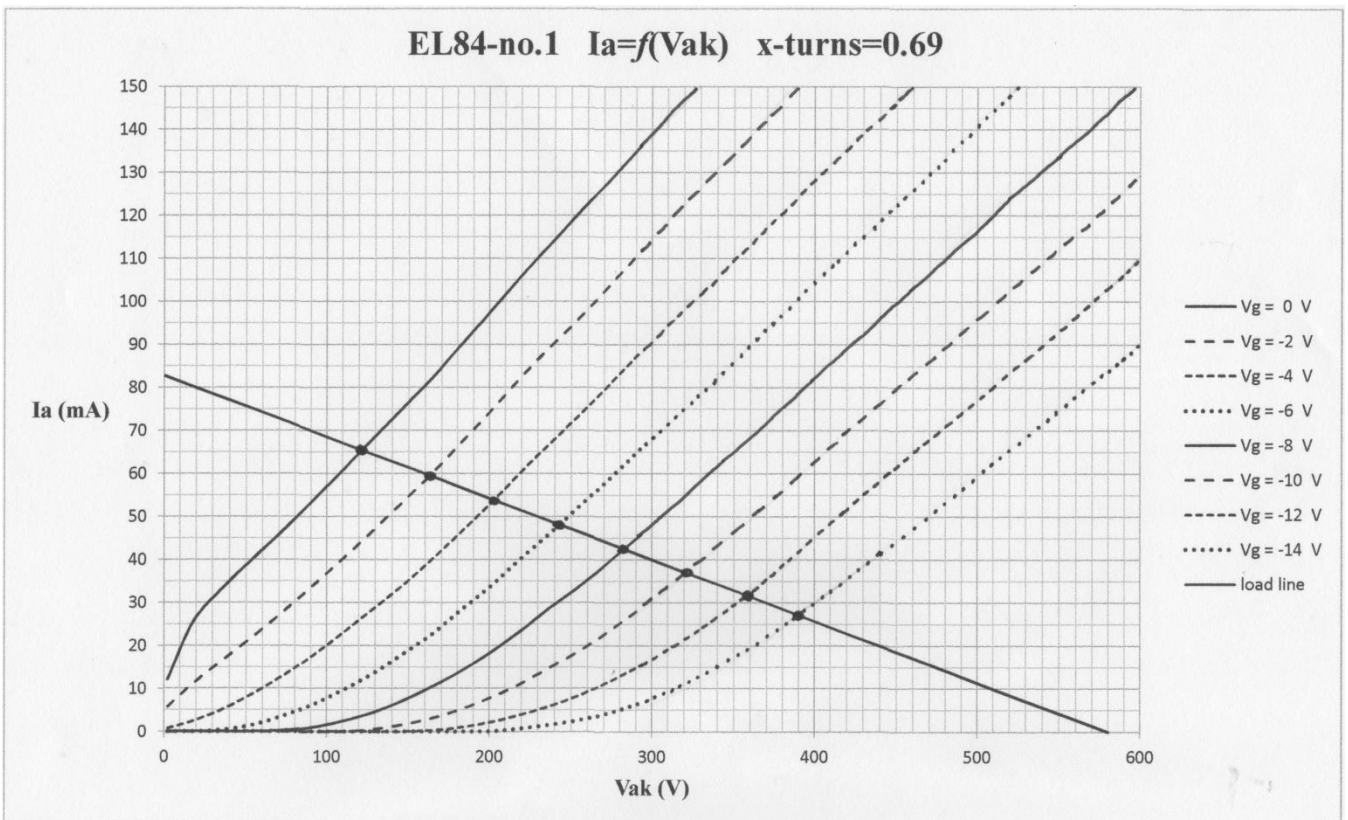
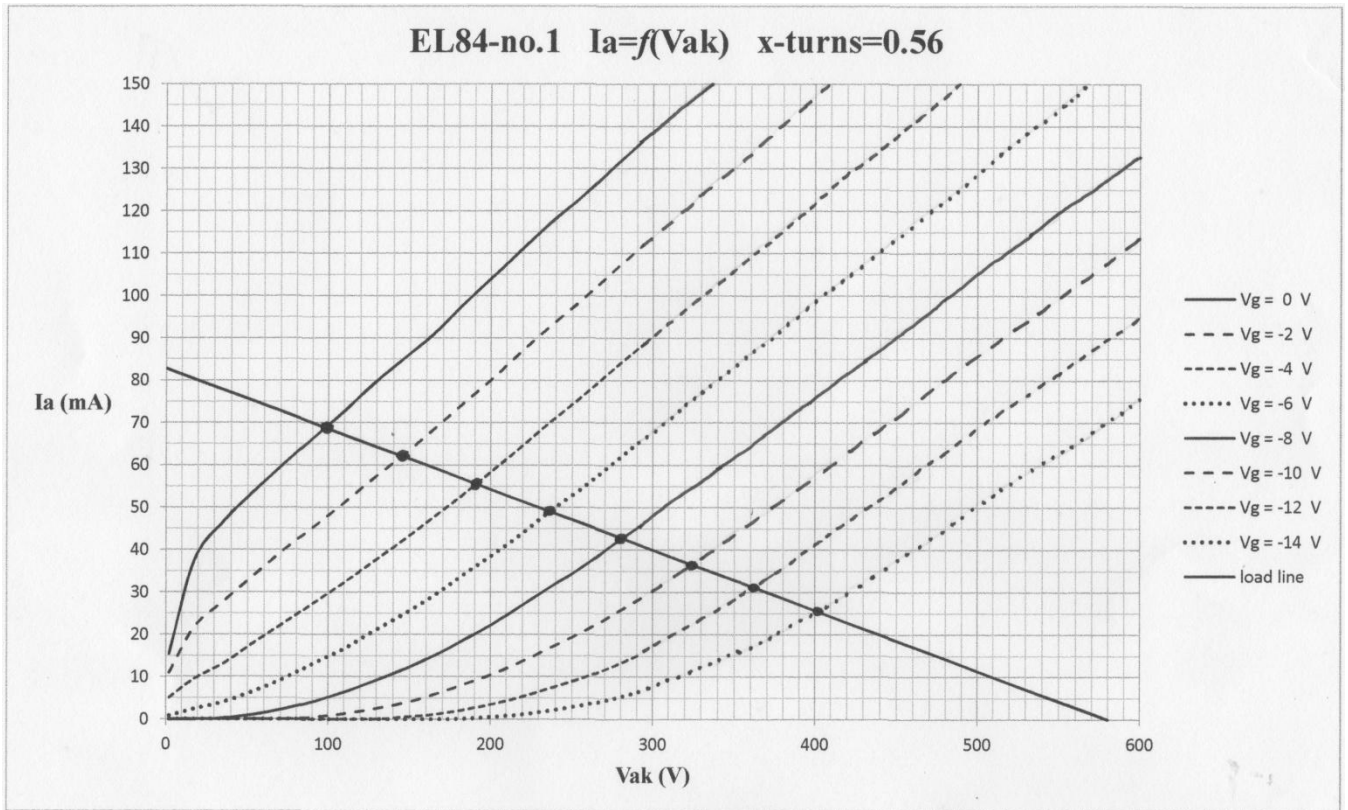
Measured with the μ Tracer and extrapolated anode characteristics of EL84 for several screen grid taps. Load line for EL84 goes through working point $V_{ak,w} = 300\text{V}$, $I_{a,w} = 40\text{mA}$ and $V_{gIk,w} \approx -9.1\text{V}$.

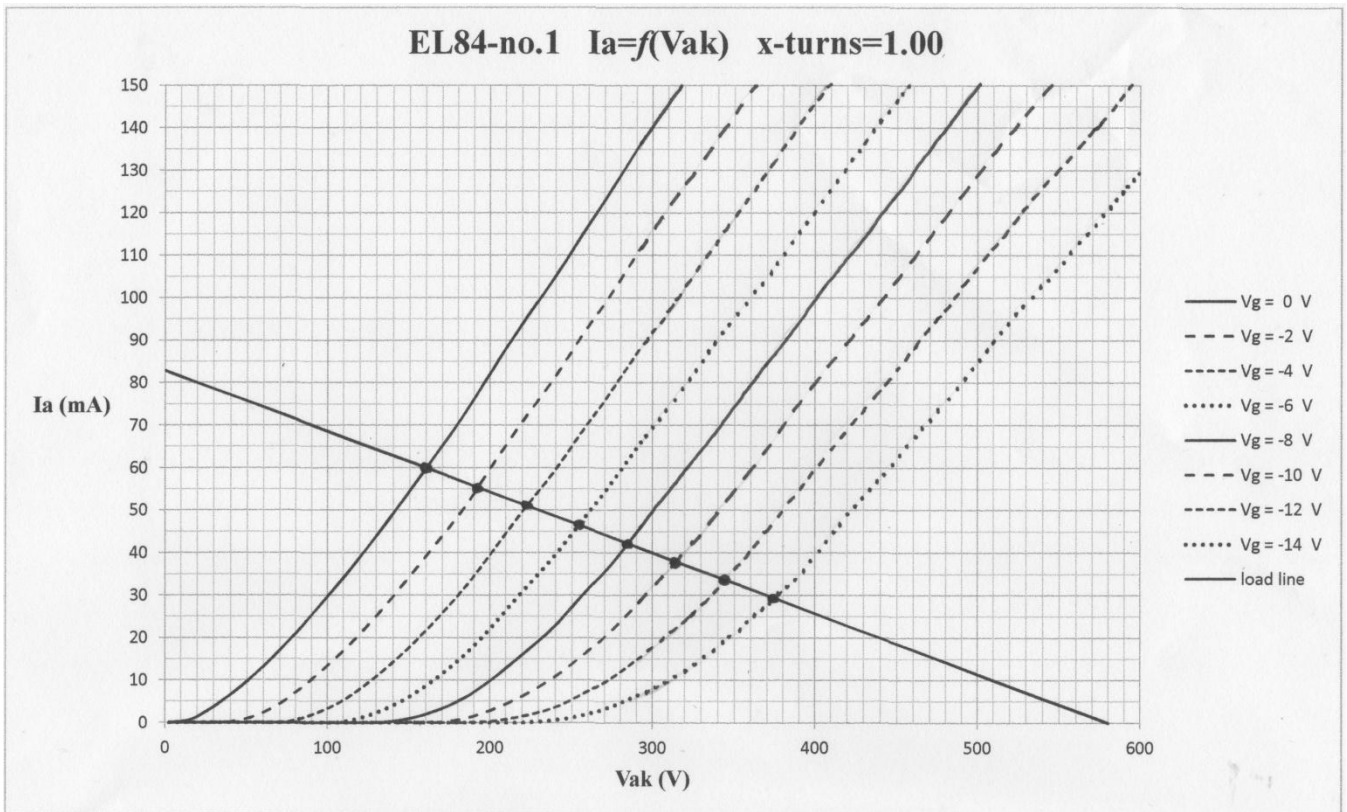






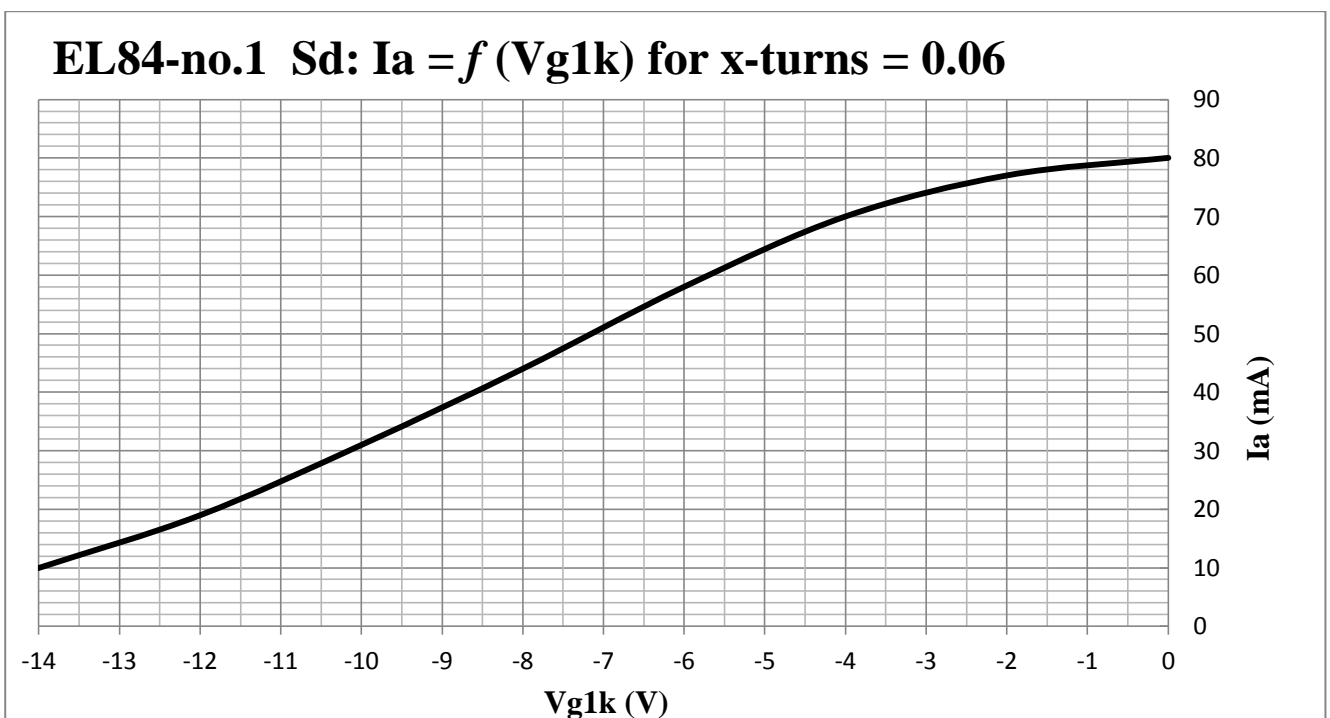
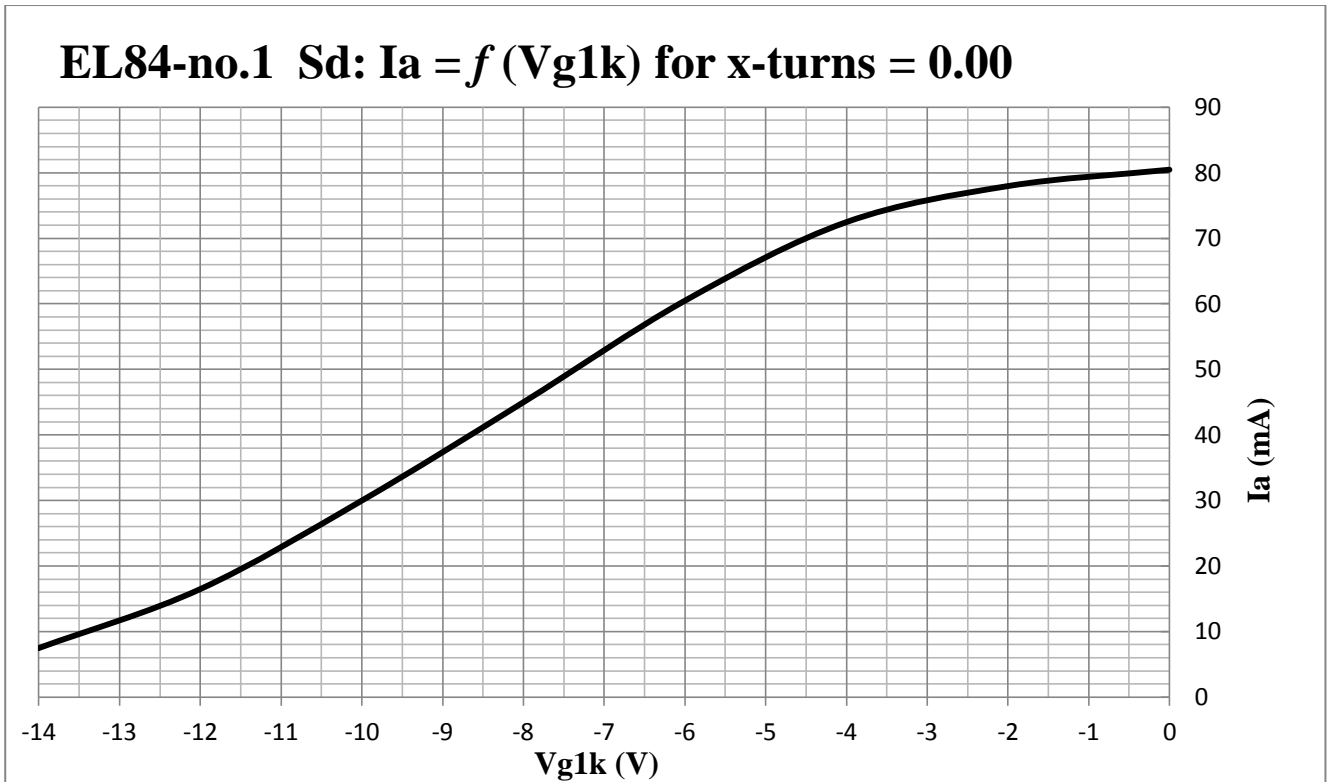


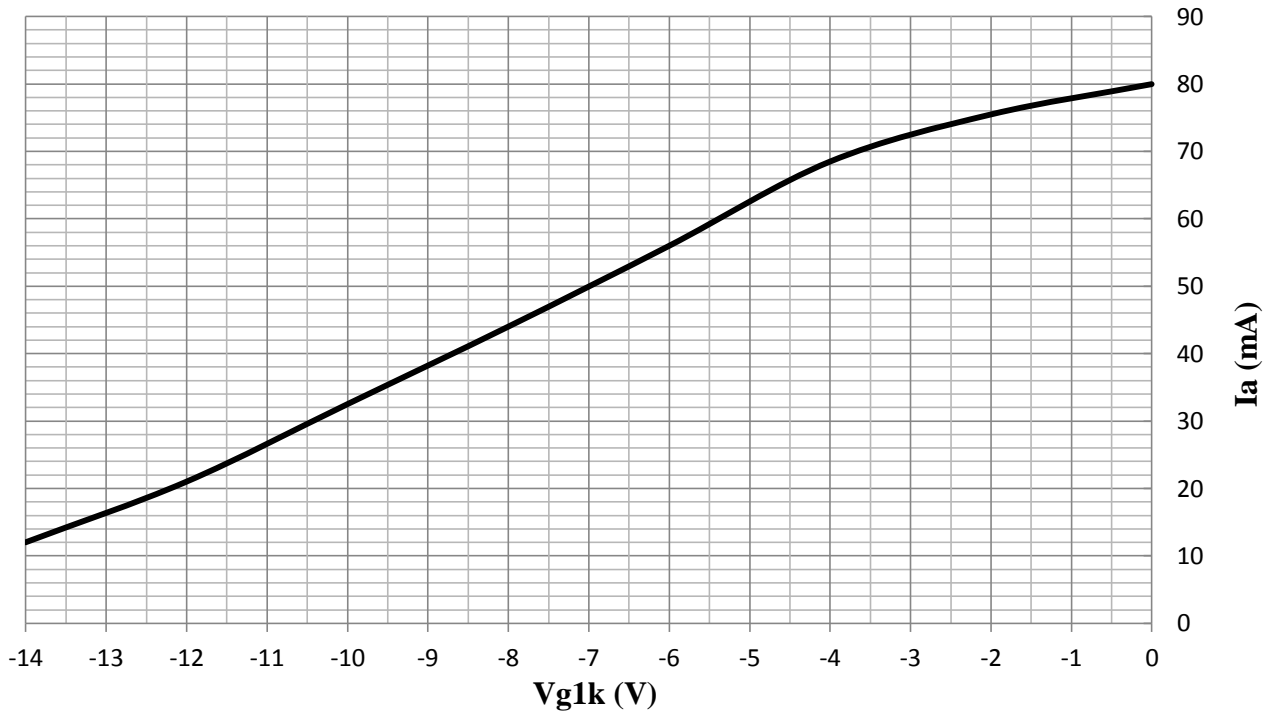
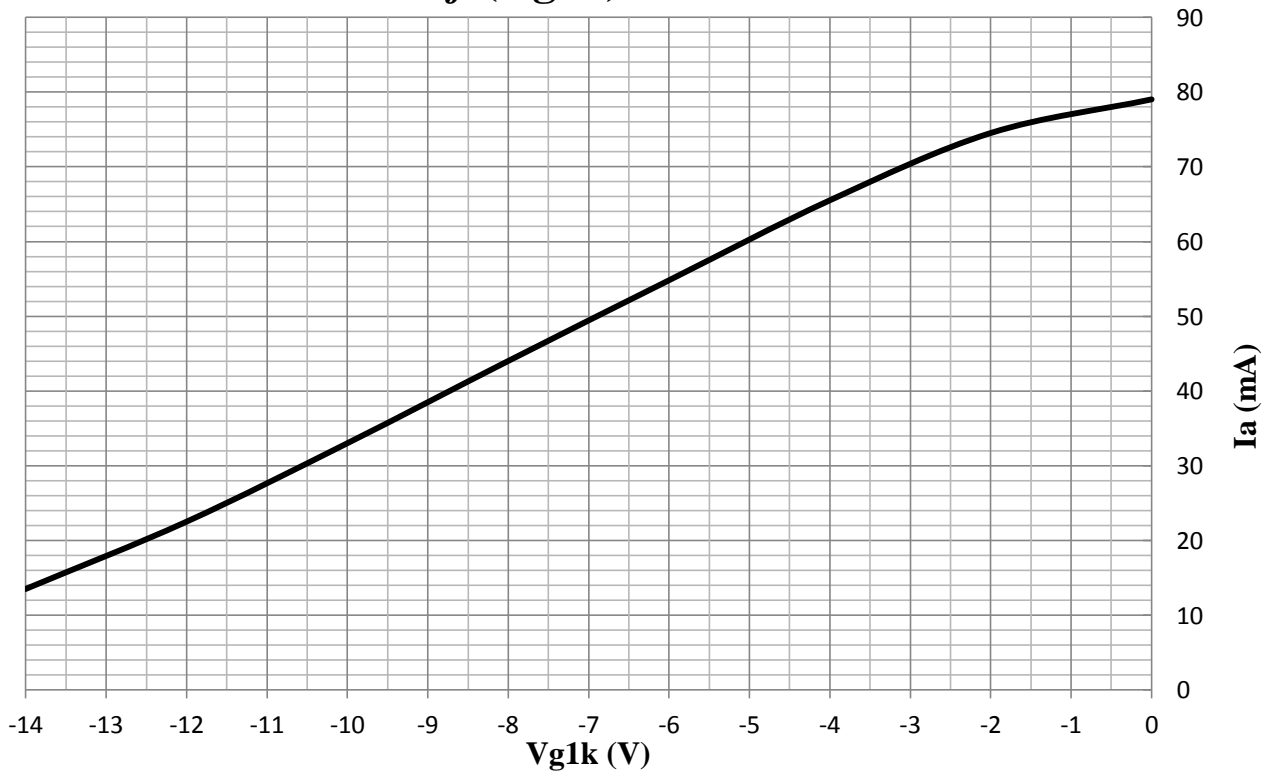


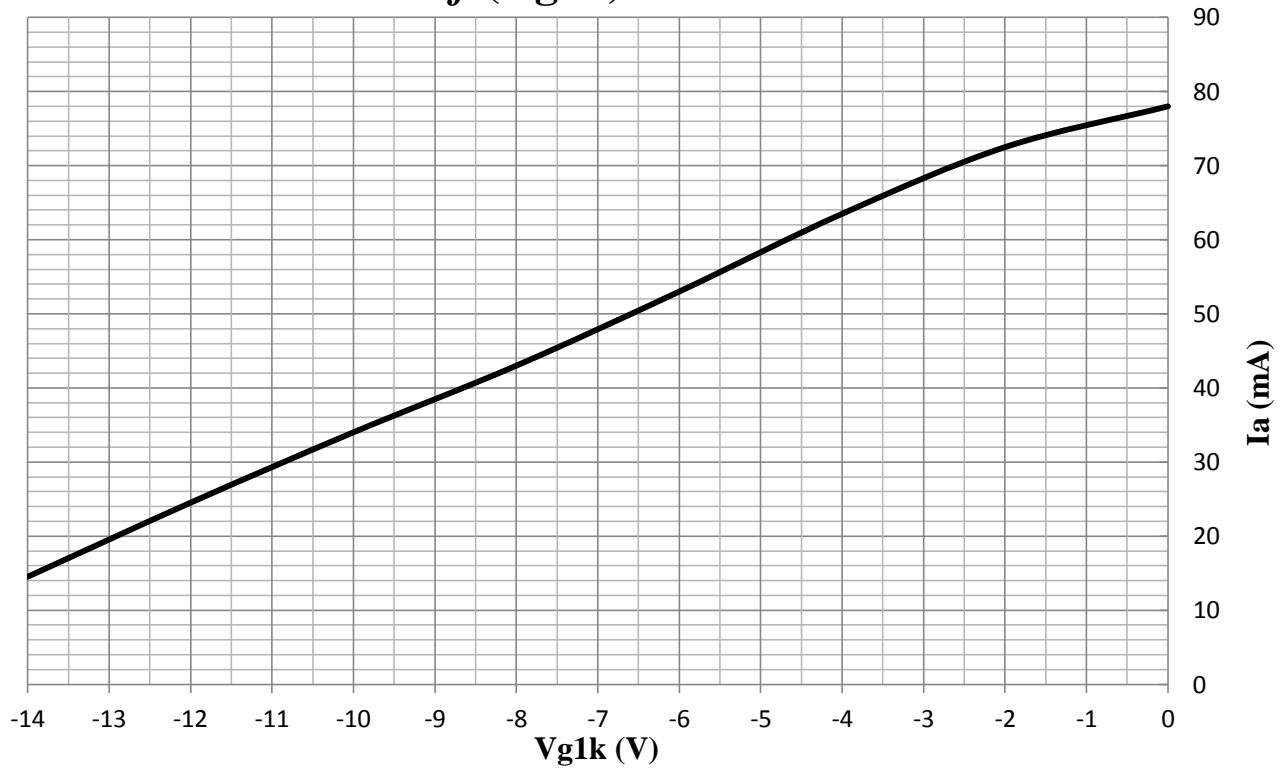
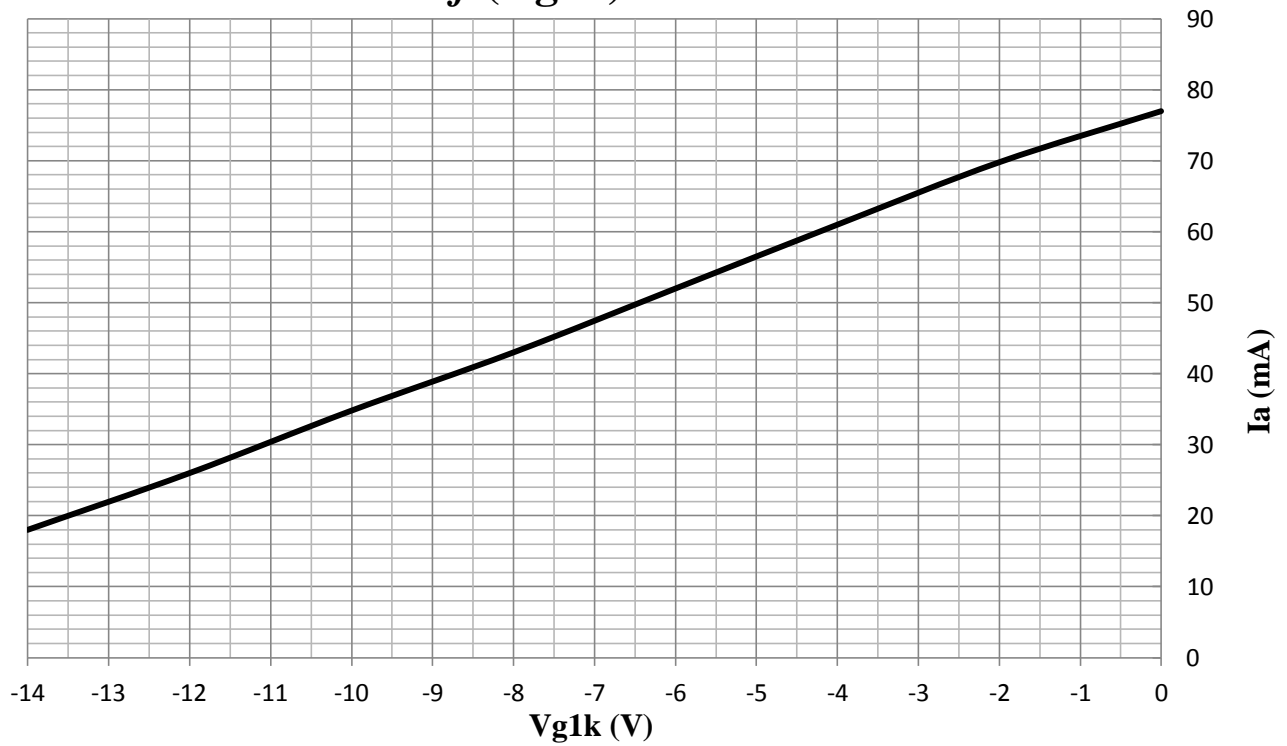


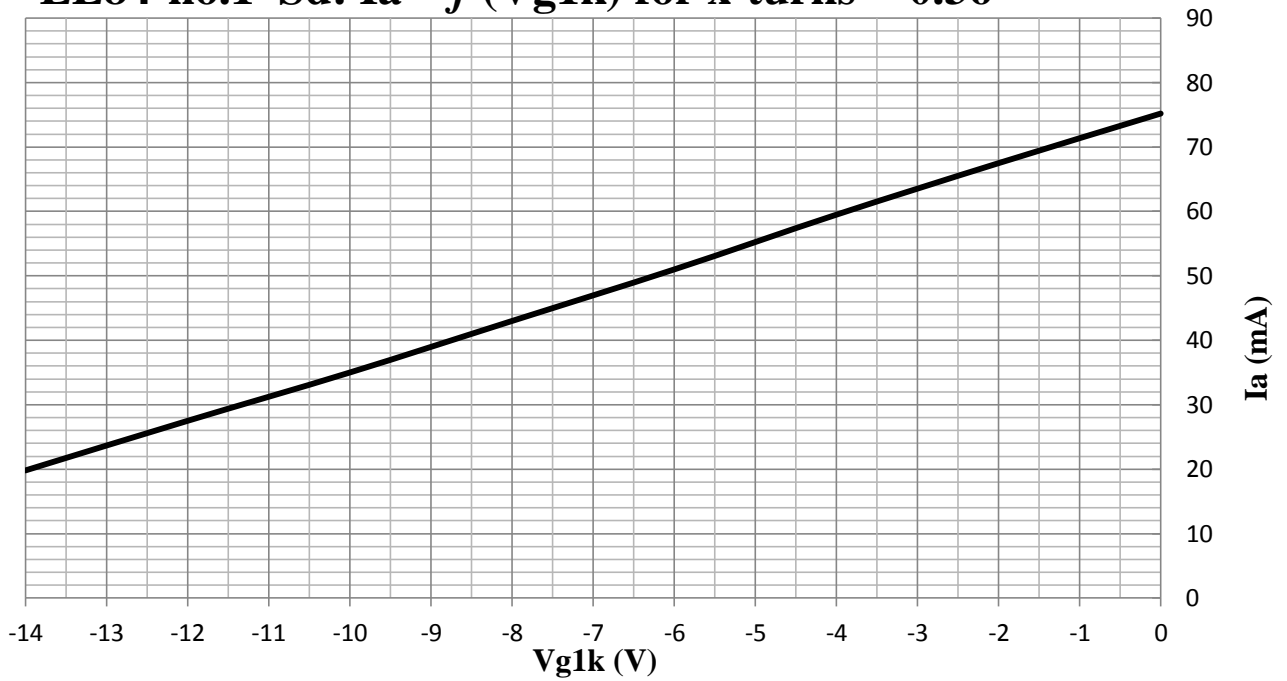
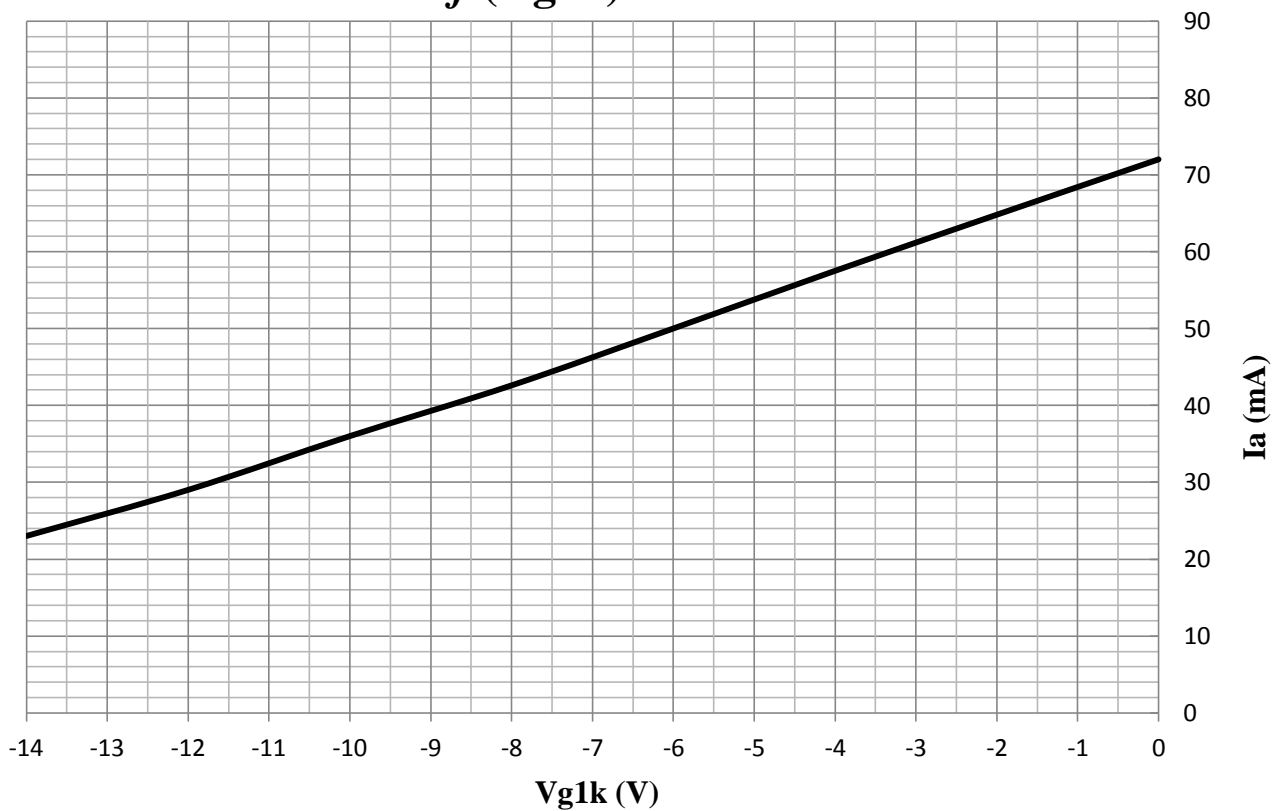
APPENDIX B

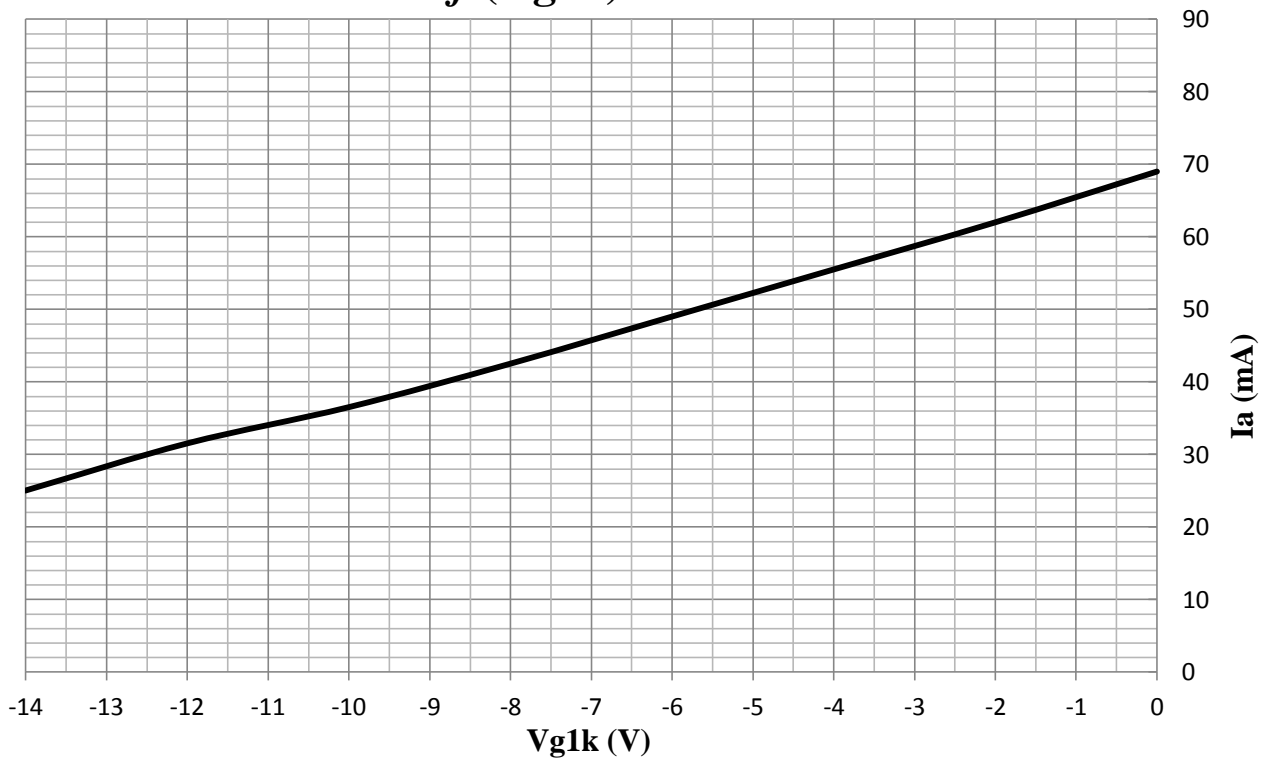
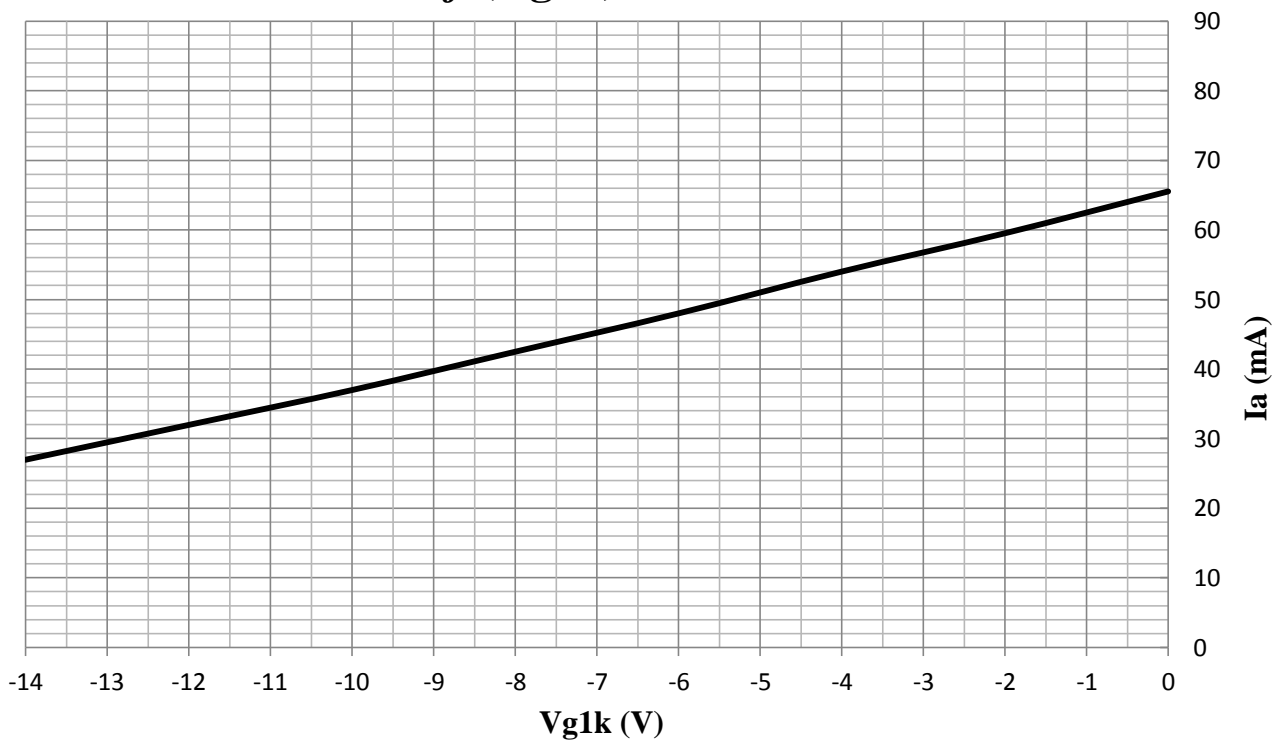
Constructed dynamic transconductance characteristics of EL84 for several screen grid taps.

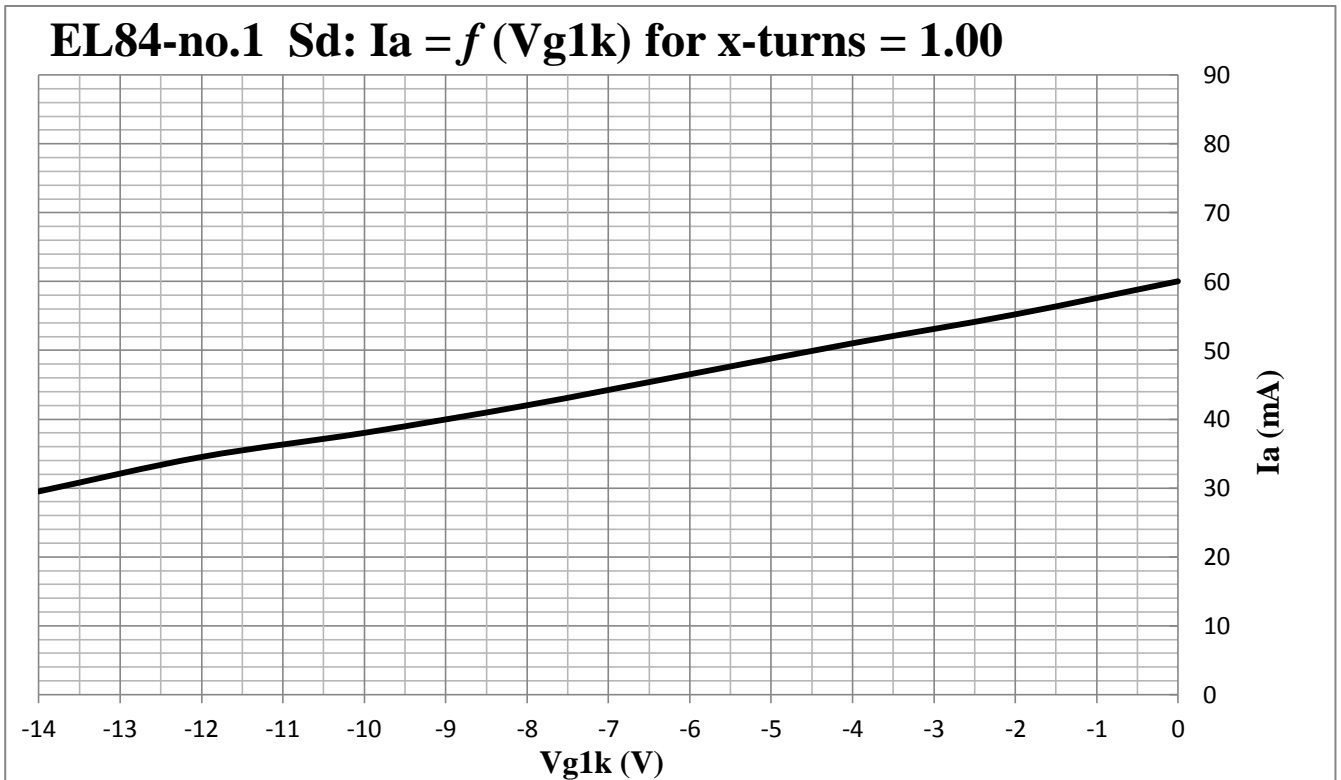


EL84-no.1 Sd: $I_a = f(V_{g1k})$ for x-turns = 0.11**EL84-no.1 Sd: $I_a = f(V_{g1k})$ for x-turns = 0.17**

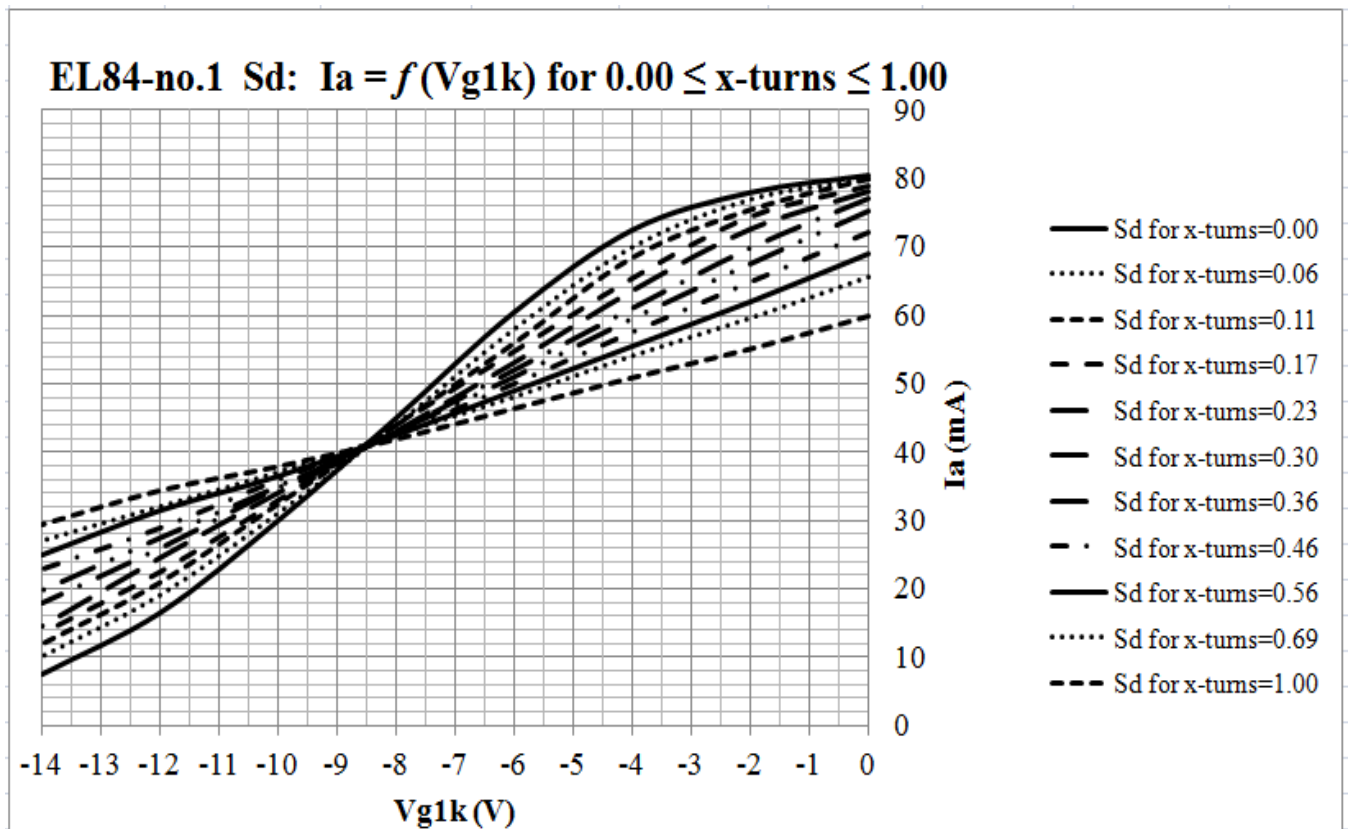
EL84-no.1 Sd: $I_a = f(V_{g1k})$ for x-turns = 0.23**EL84-no.1 Sd: $I_a = f(V_{g1k})$ for x-turns = 0.30**

EL84-no.1 Sd: $I_a = f(V_{g1k})$ for x-turns = 0.36**EL84-no.1 Sd: $I_a = f(V_{g1k})$ for x-turns = 0.46**

EL84-no.1 Sd: $I_a = f(V_{g1k})$ for x-turns = 0.56**EL84-no.1 Sd: $I_a = f(V_{g1k})$ for x-turns = 0.69**

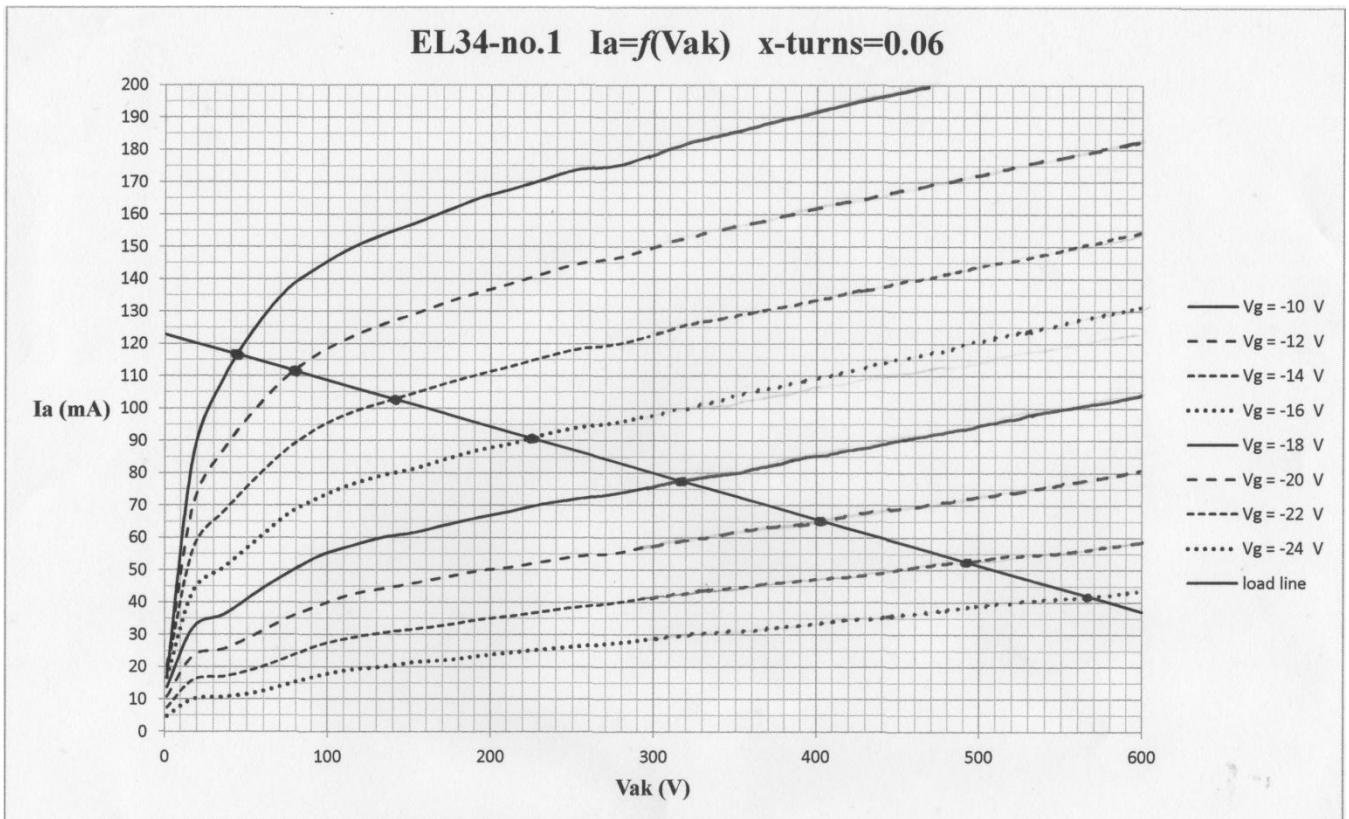
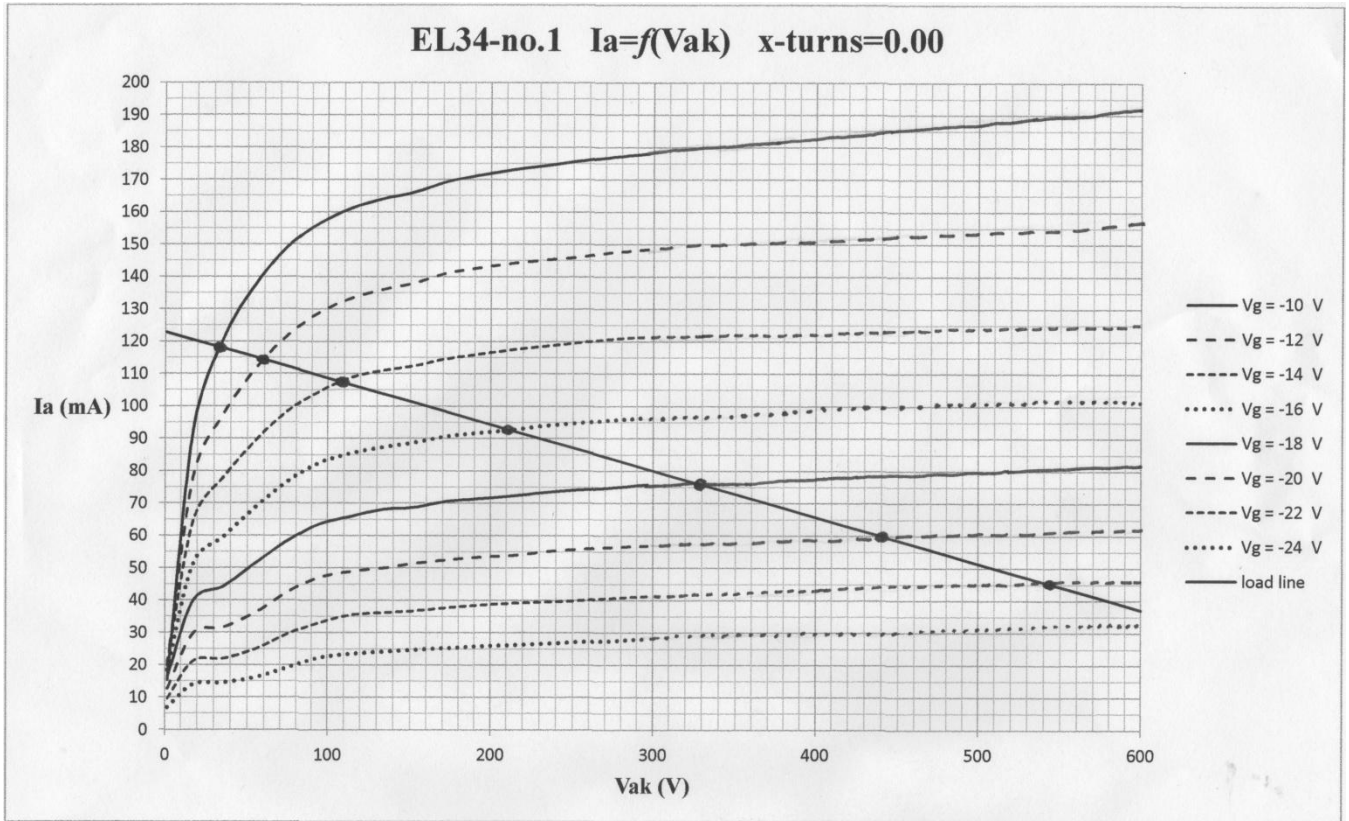


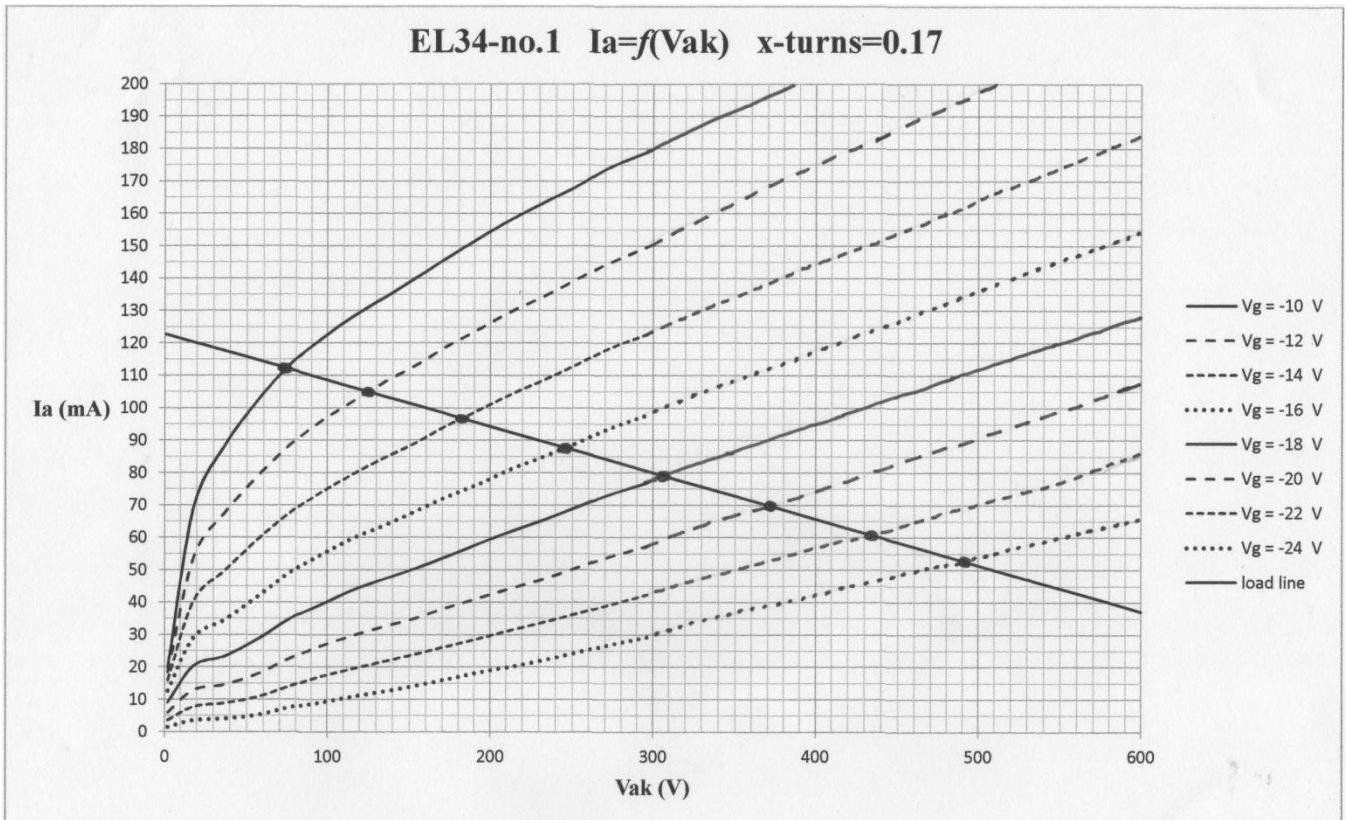
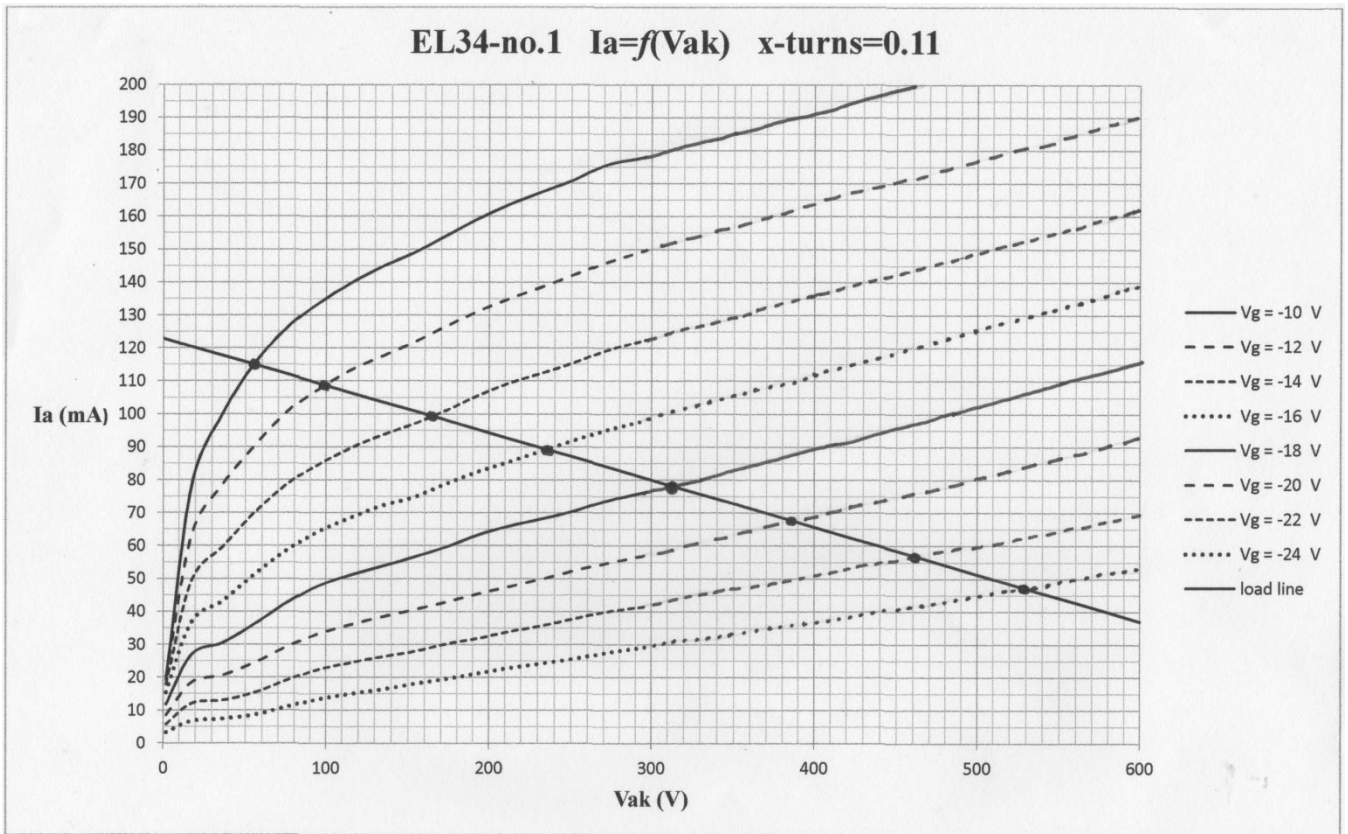
And finally all these S_d together in one transconductance characteristic.

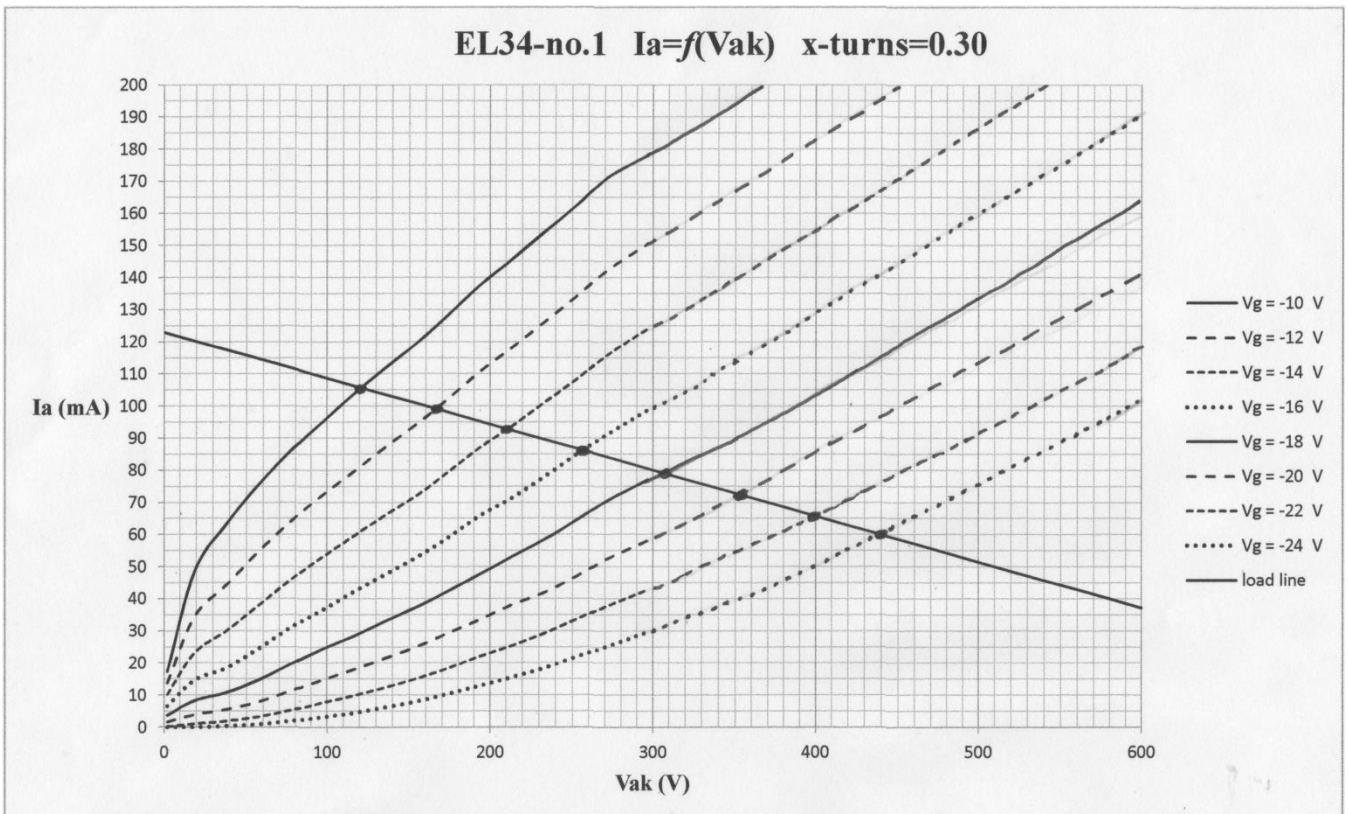
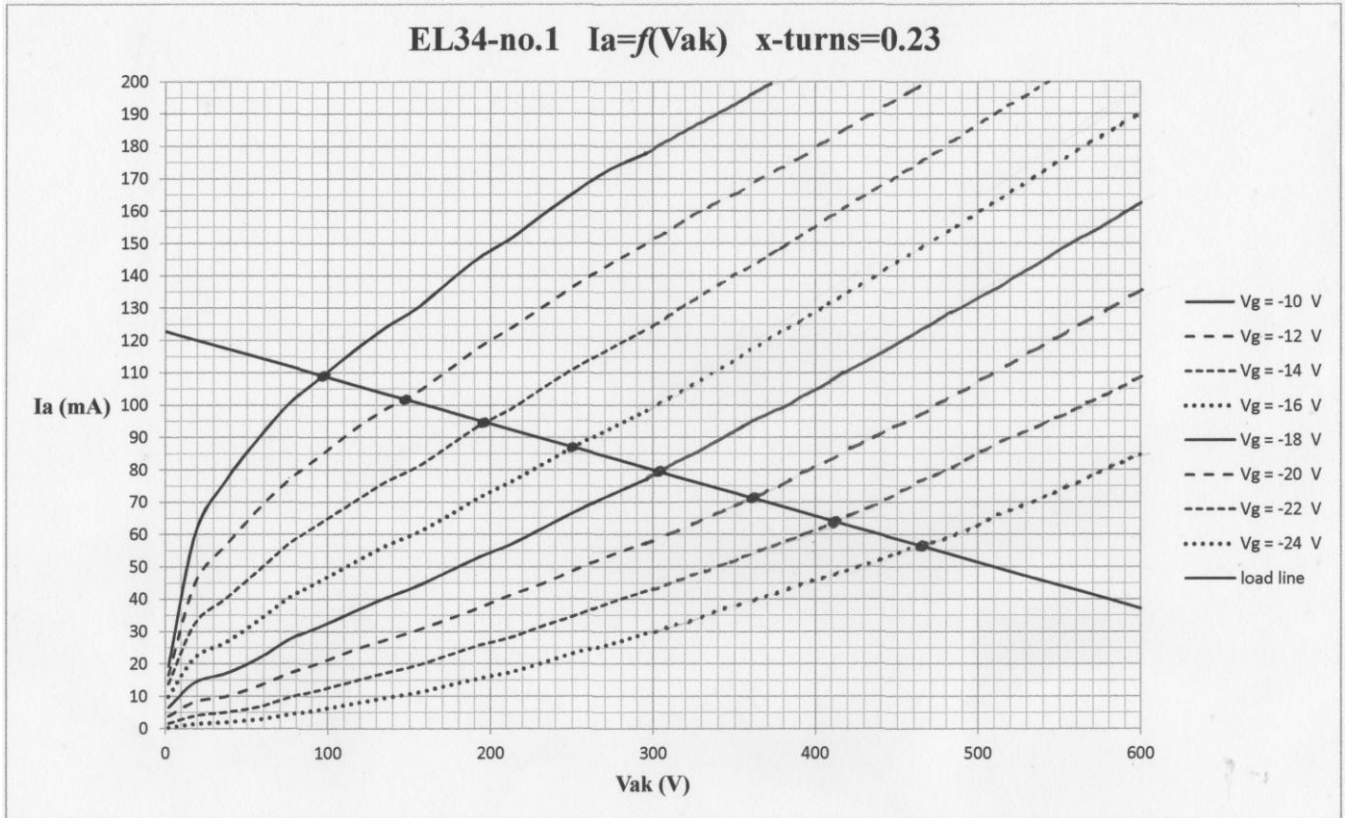


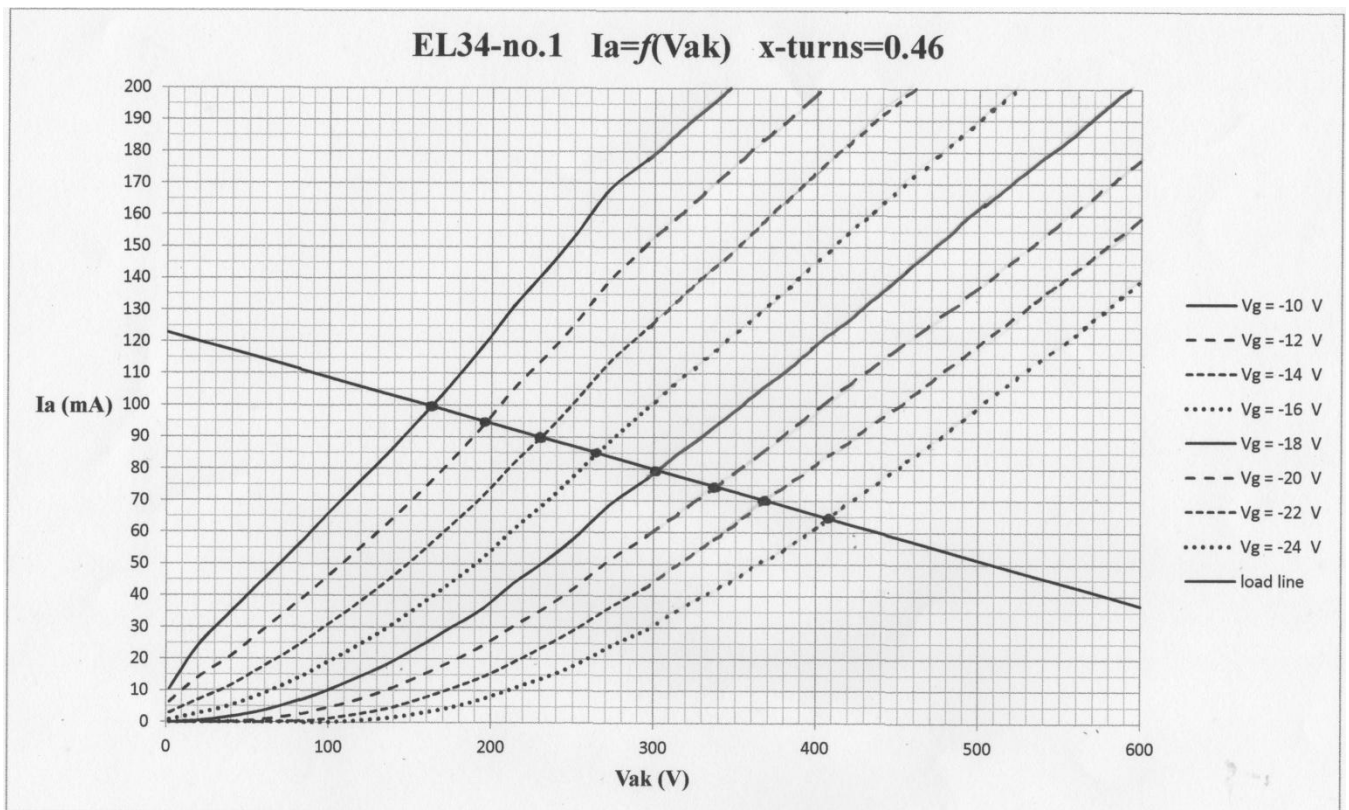
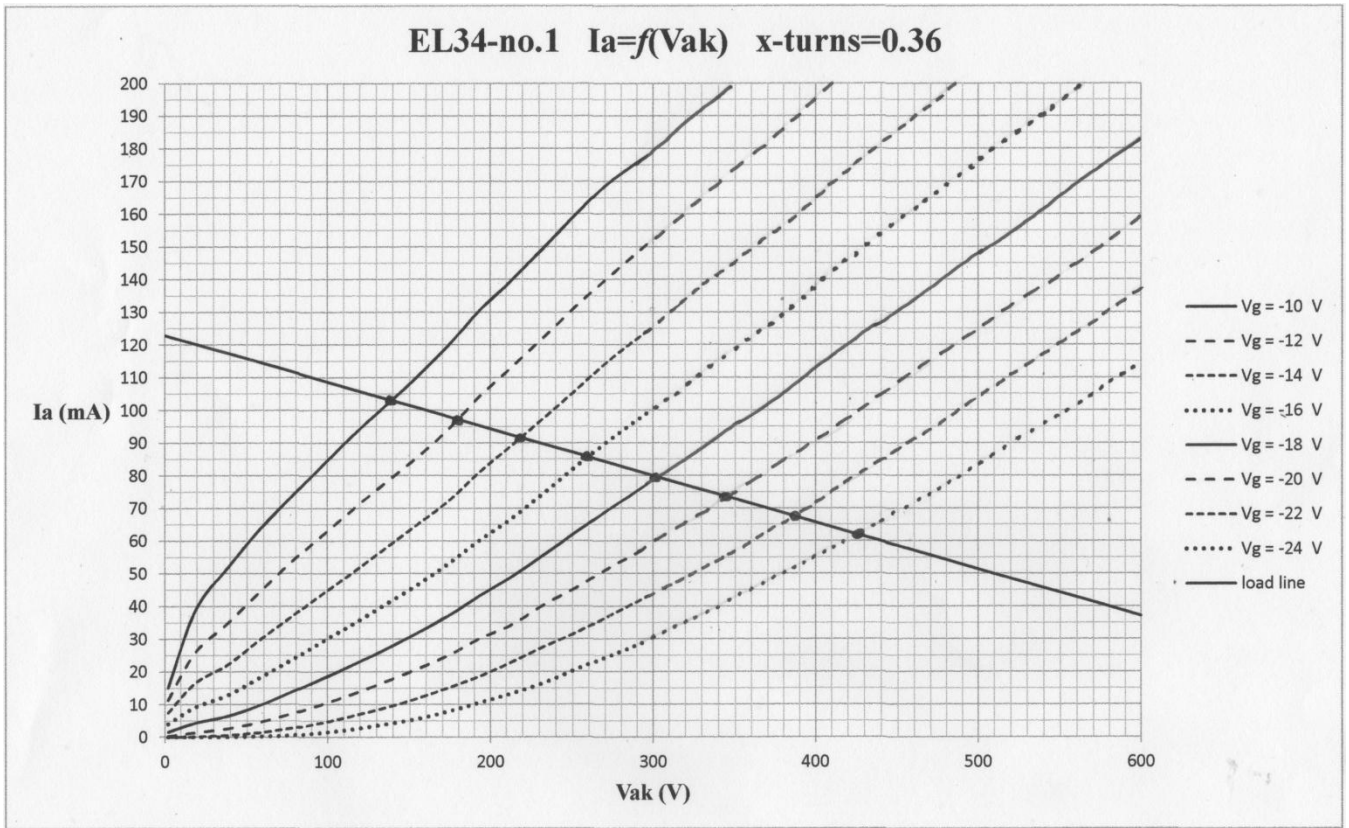
APPENDIX C

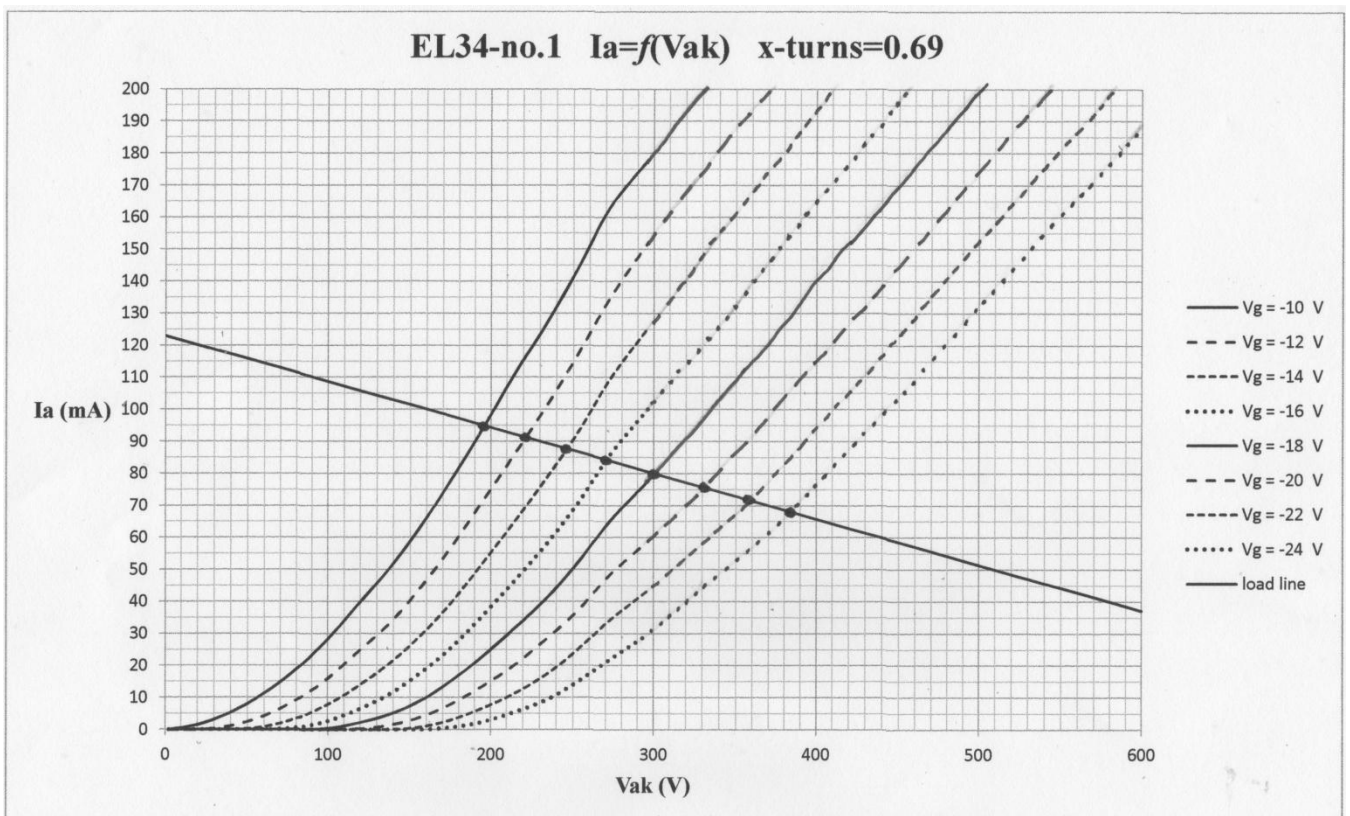
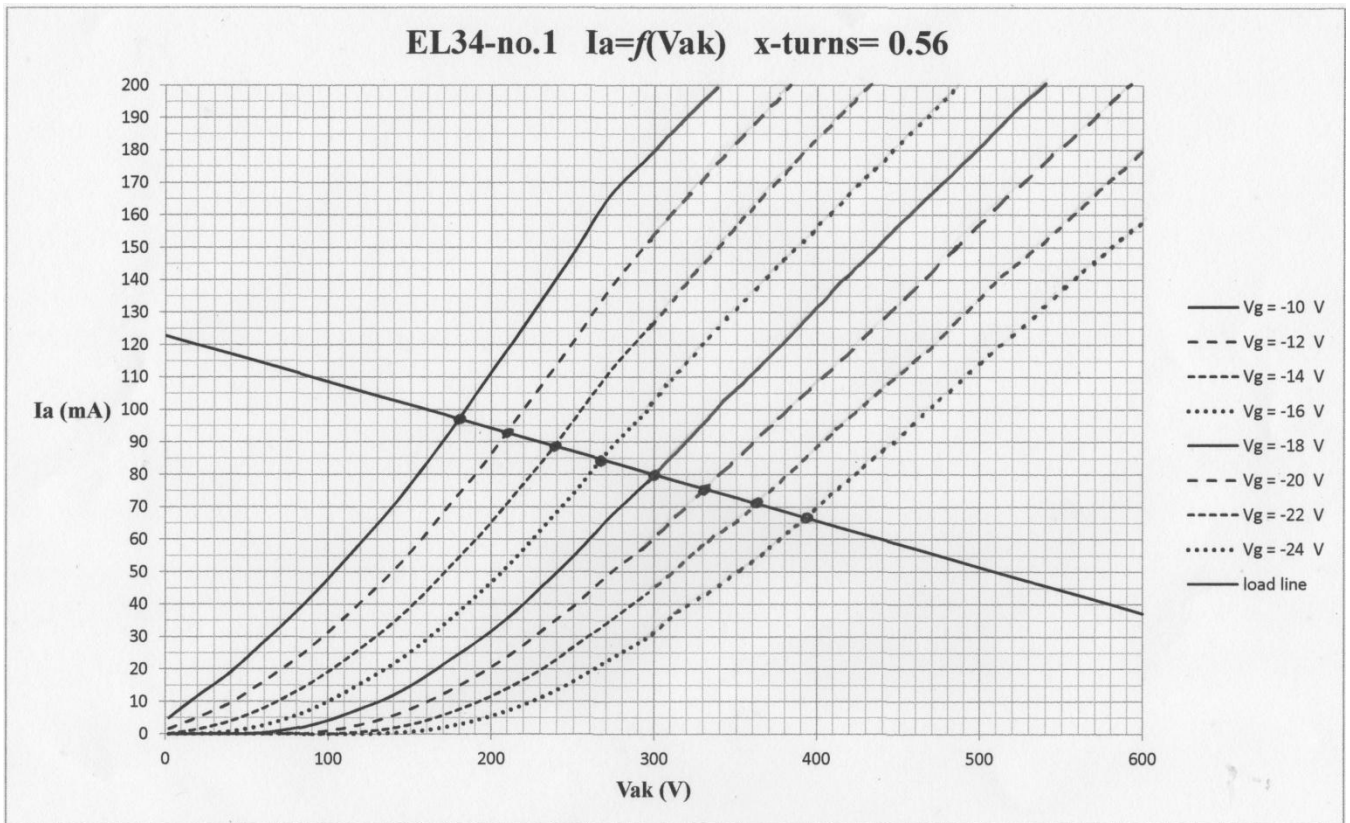
Measured with the μ Tracer and extrapolated anode characteristics of EL34 for several screen grid taps. Load line for EL34 goes through working point $V_{ak,w} = 300\text{V}$, $I_{a,w} = 80\text{mA}$ and $V_{gIk,w} \approx -16.1\text{V}$.





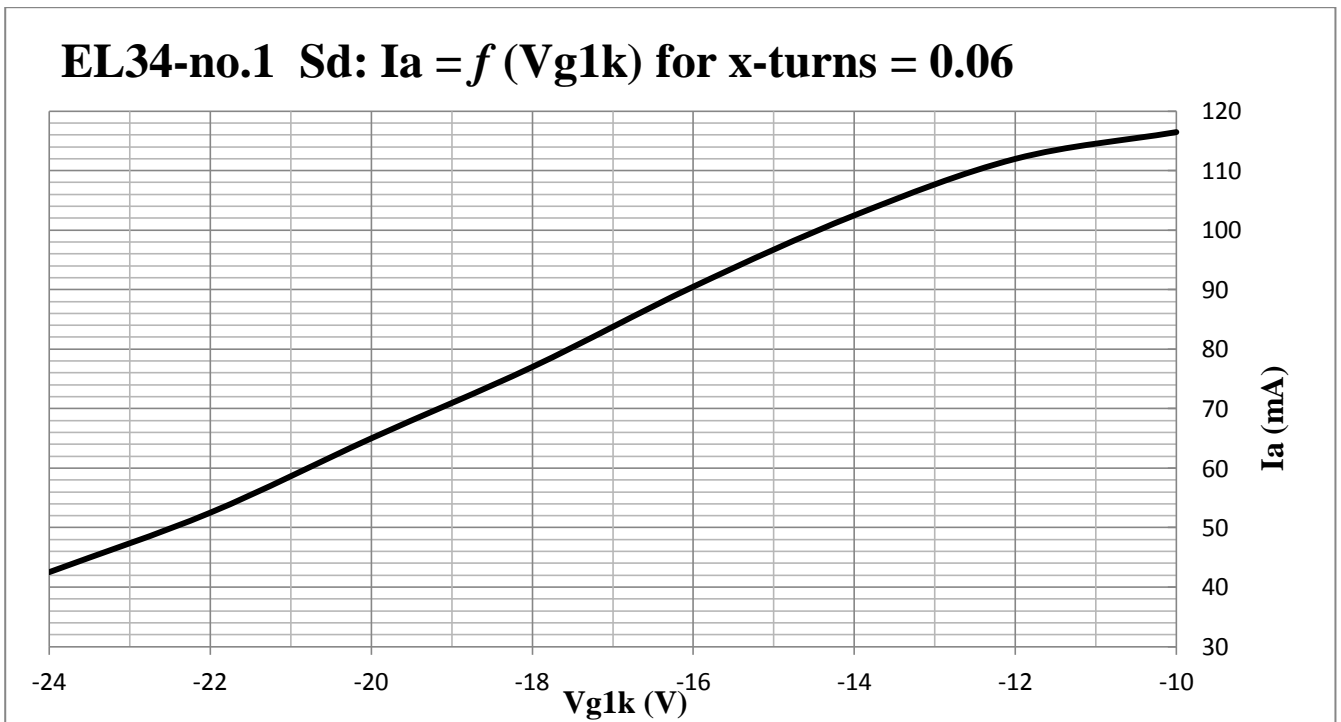
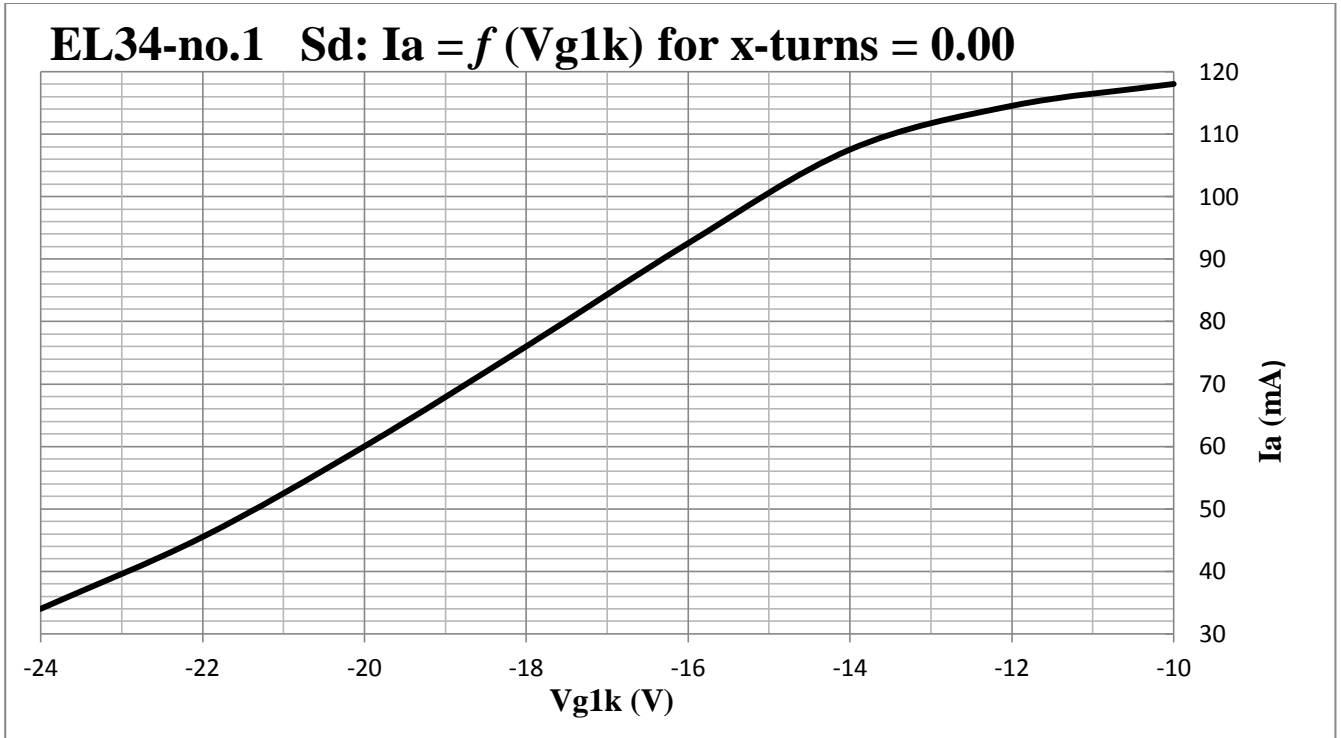


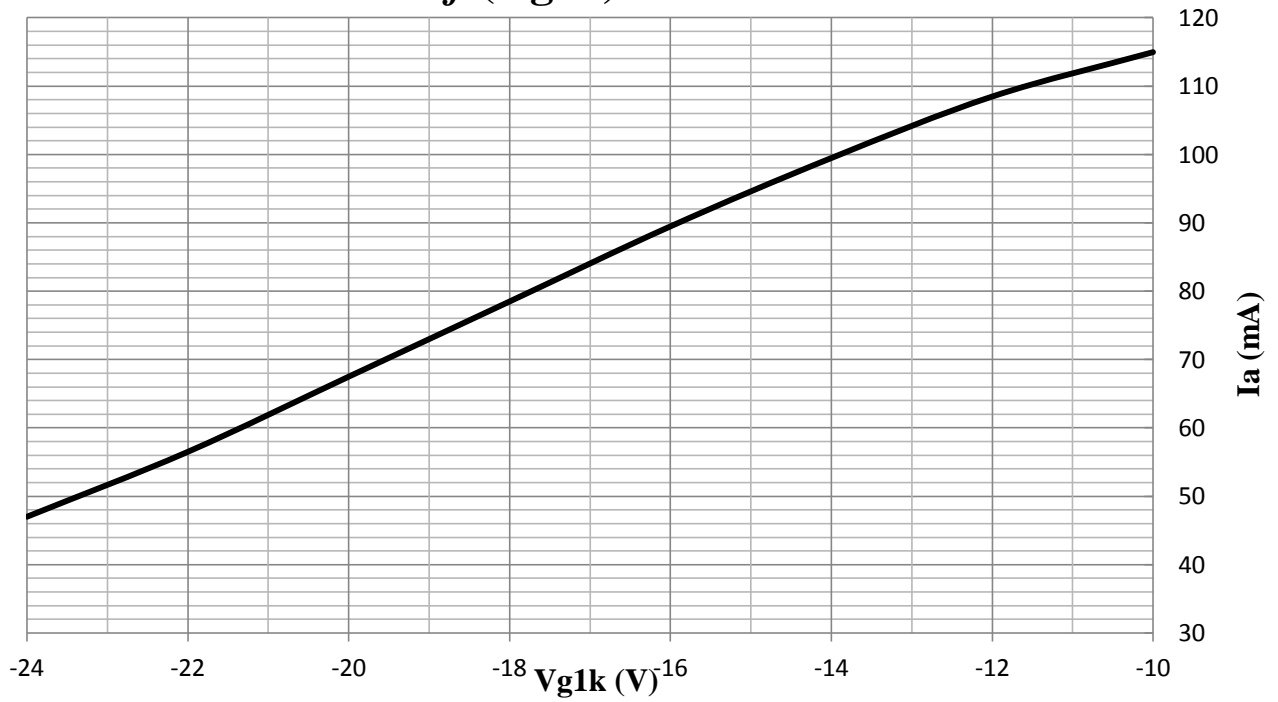
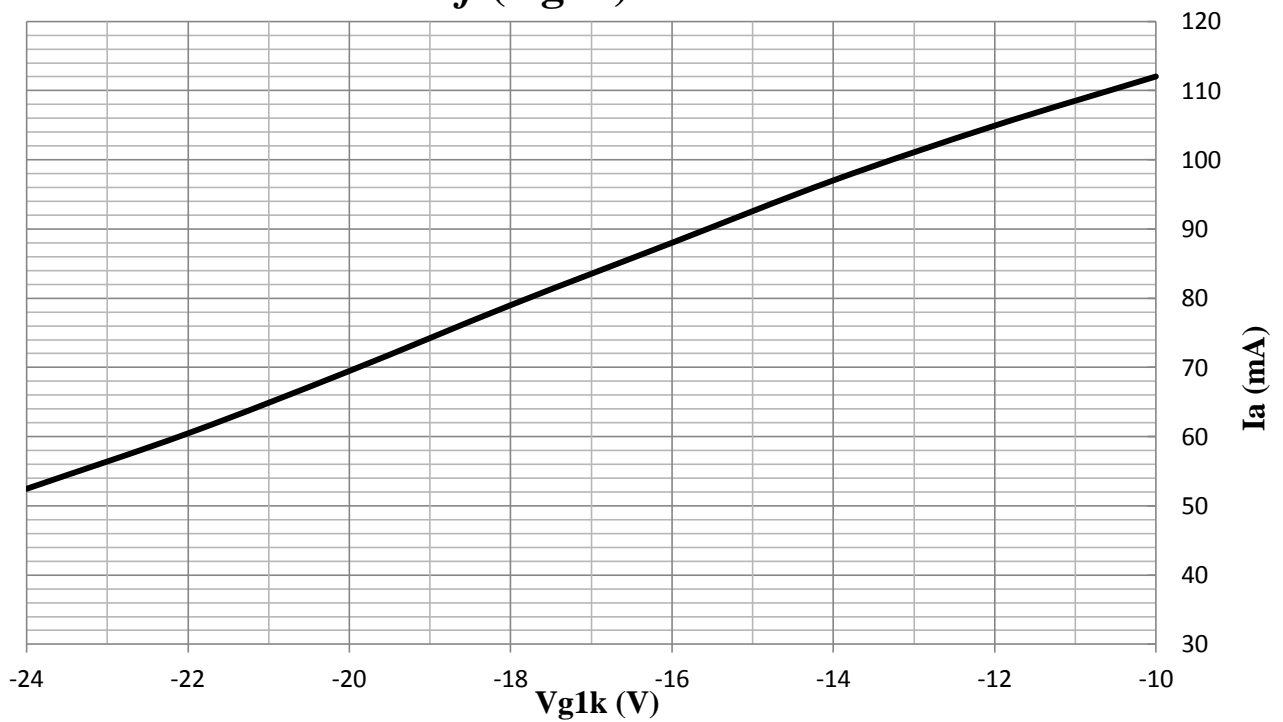


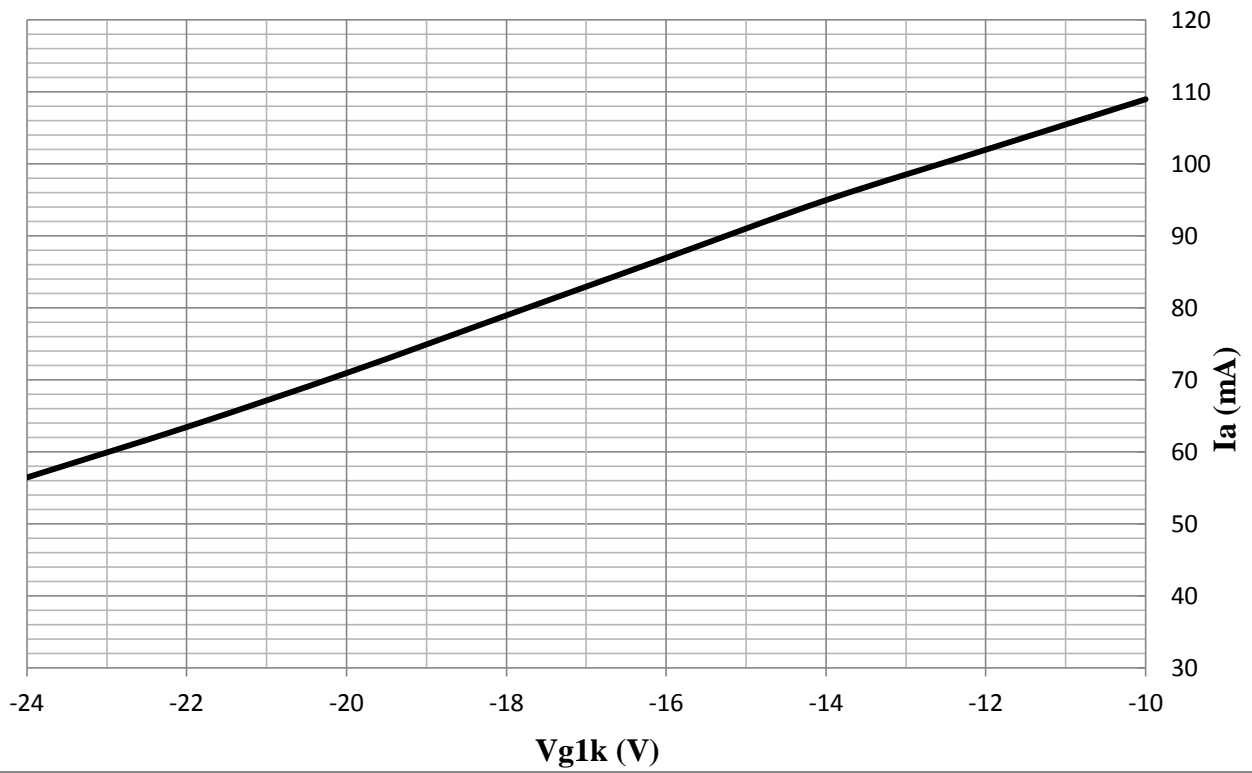
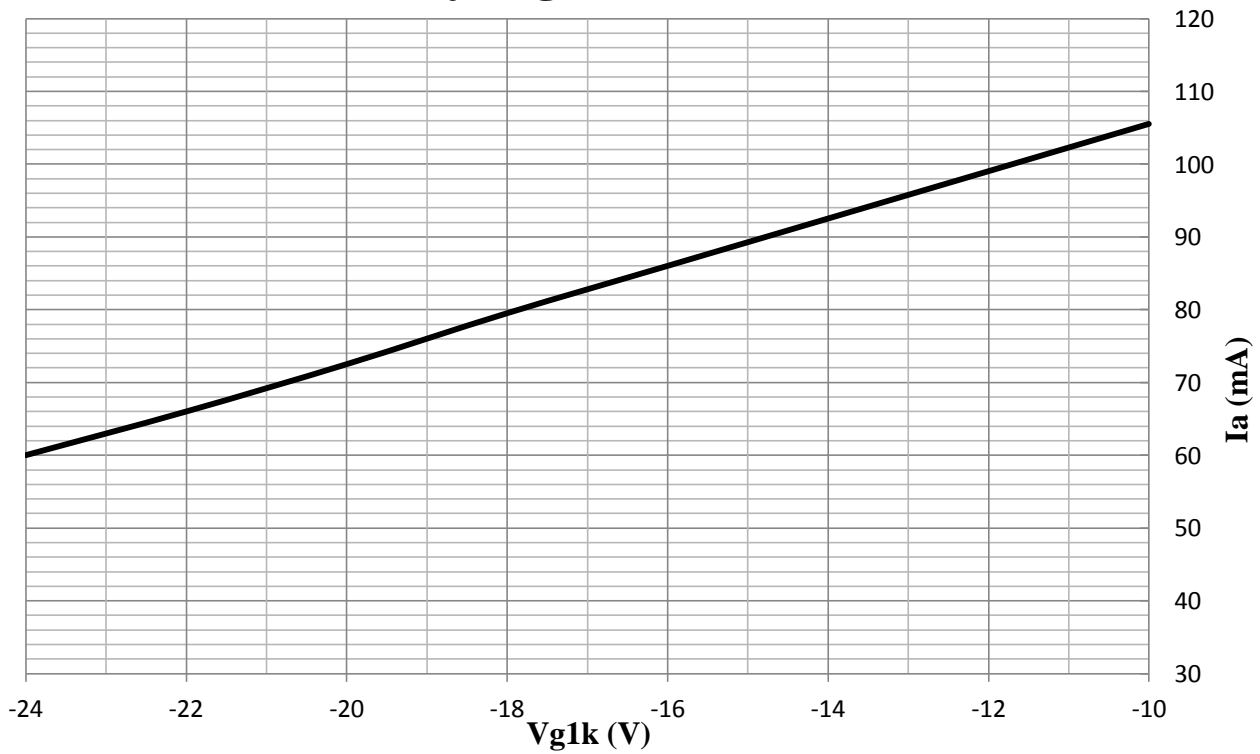


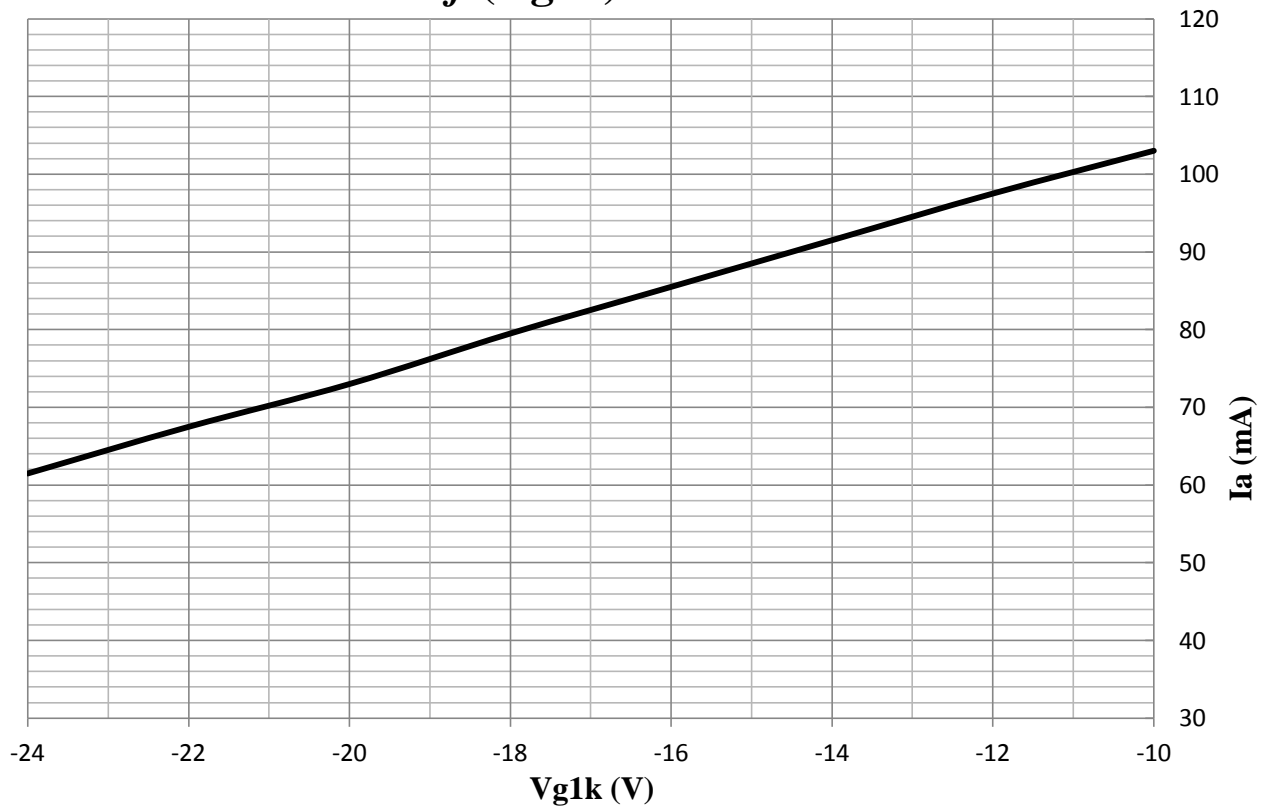
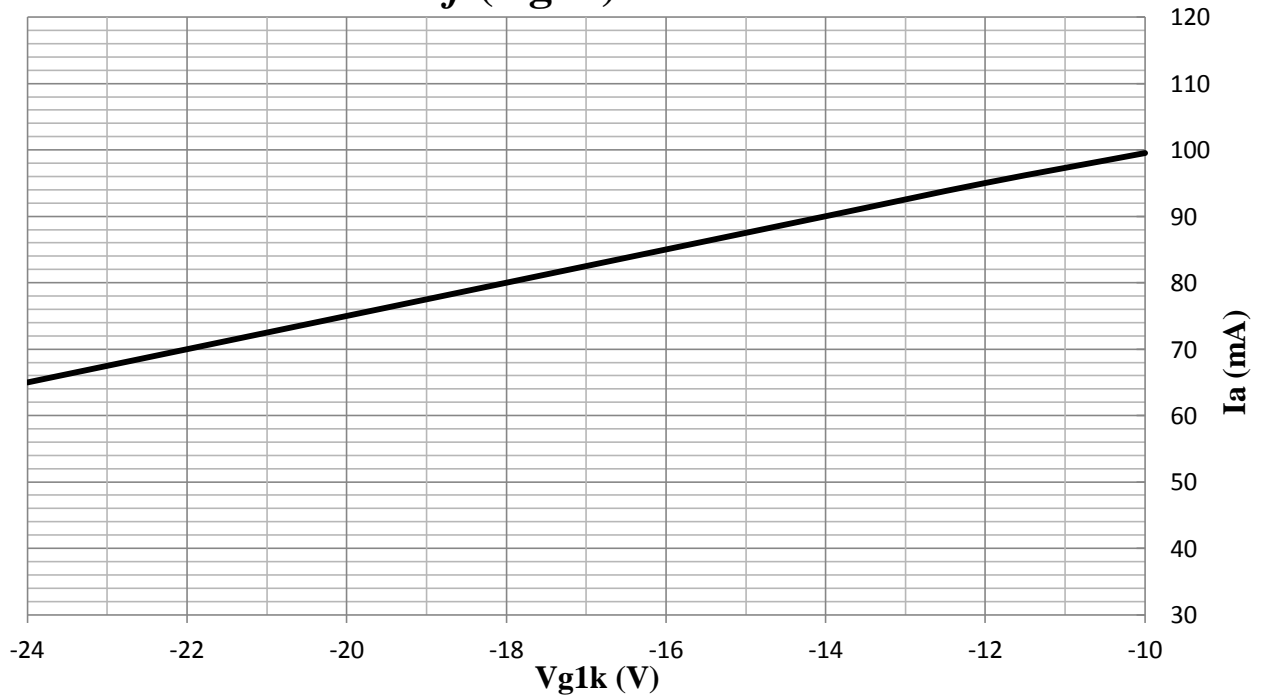
APPENDIX D

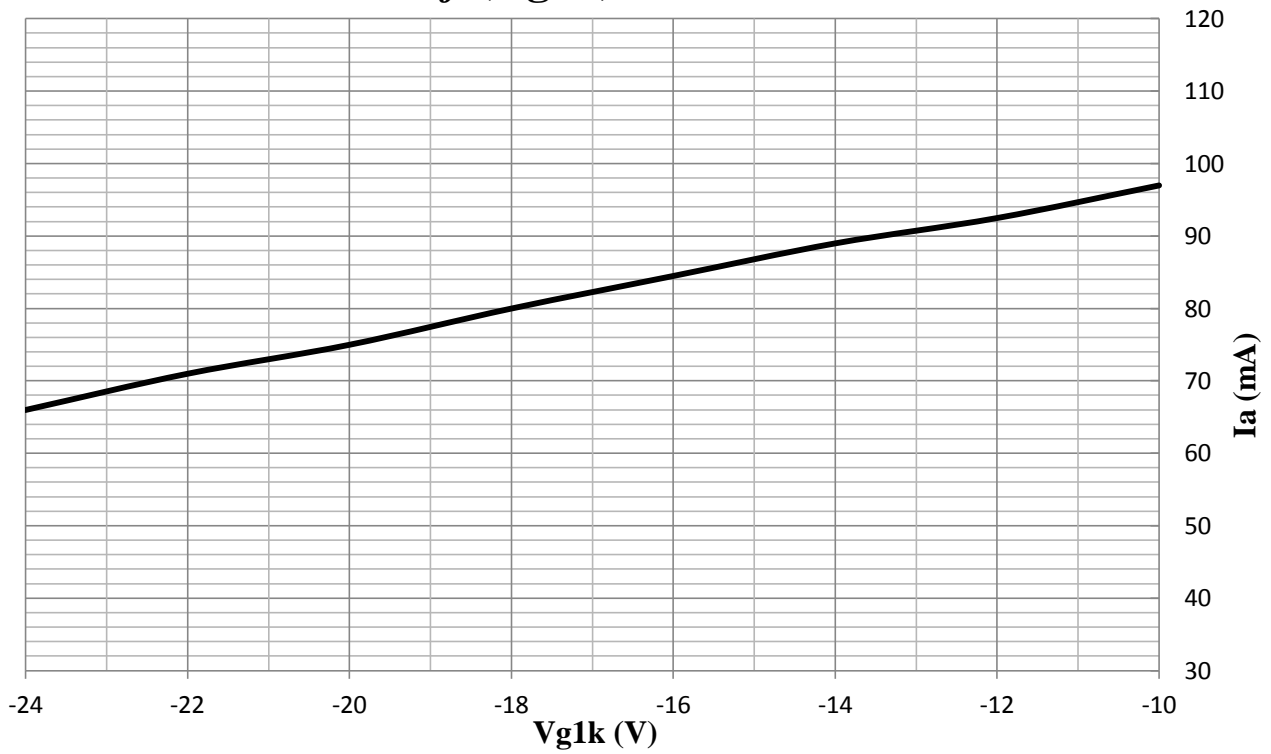
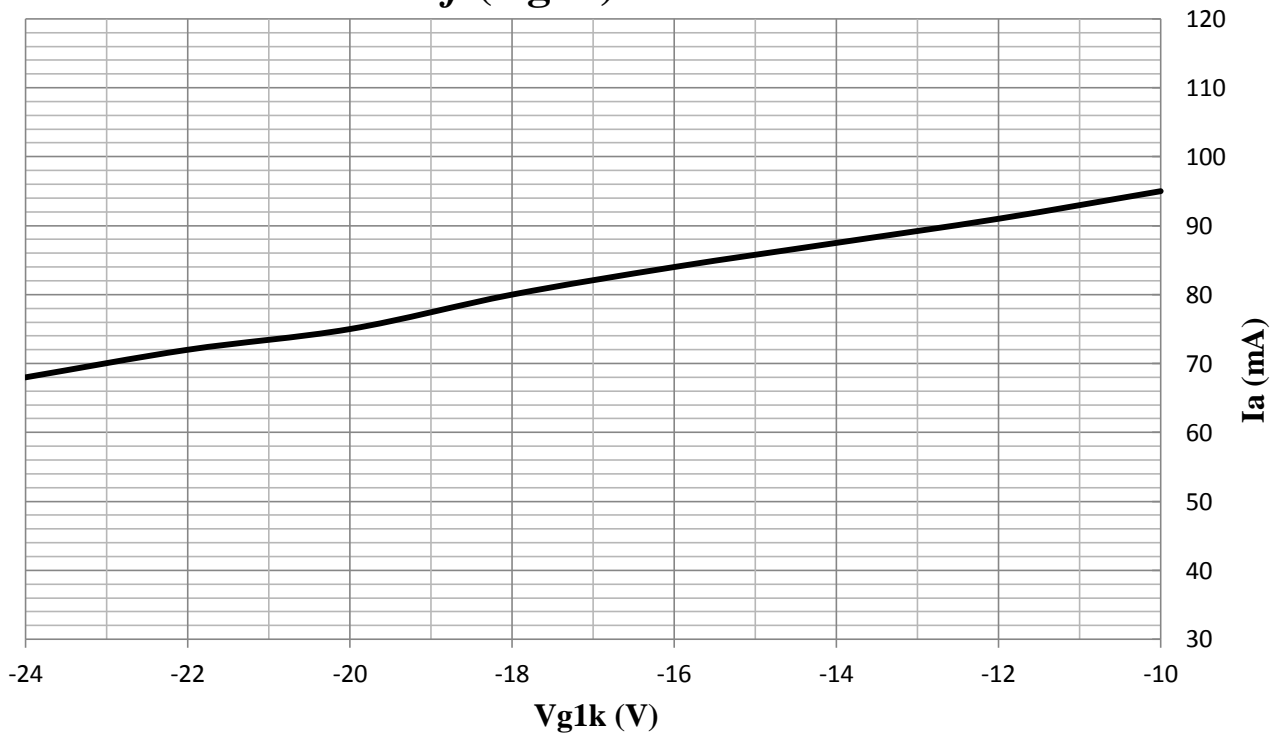
Constructed dynamic transconductance characteristics of EL34 for several screen grid taps.

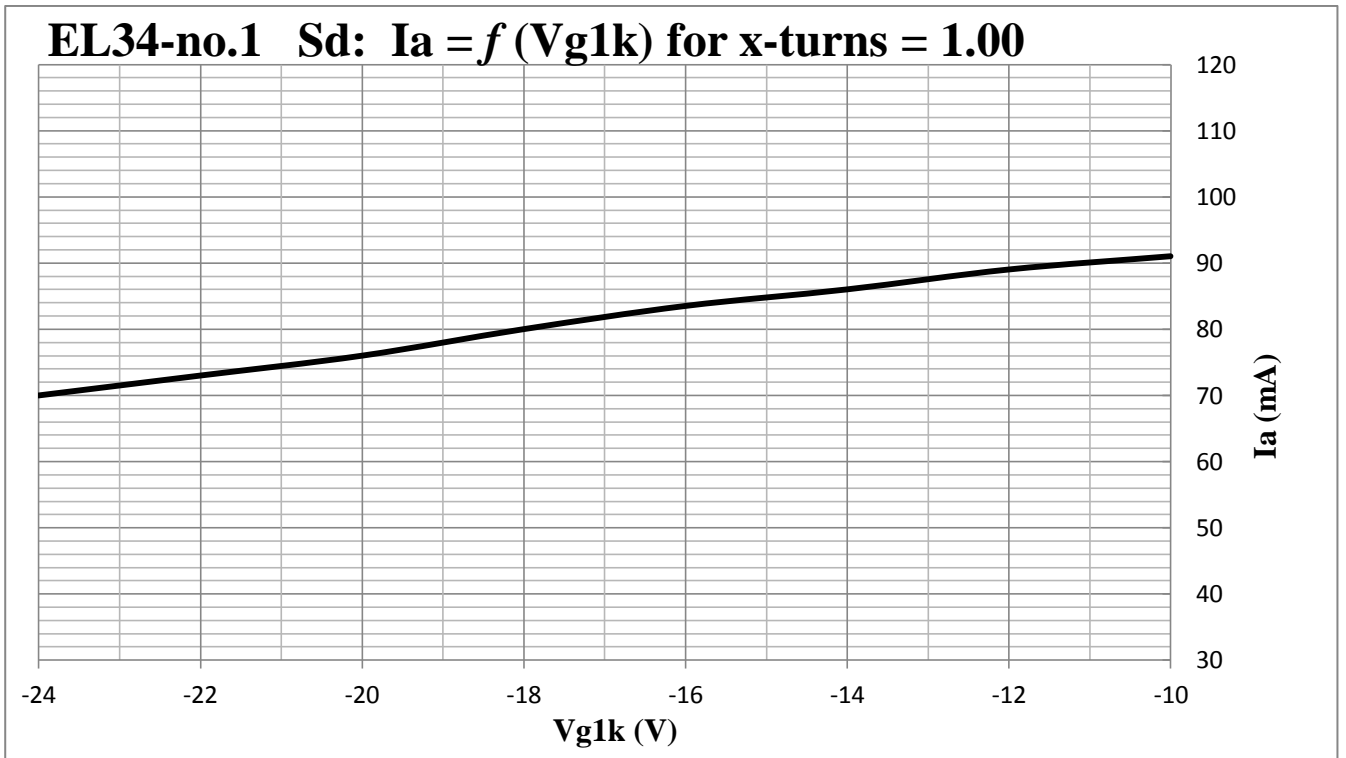


EL34-no.1 Sd: $I_a = f(V_{g1k})$ for x-turns = 0.11**EL34-no.1 Sd: $I_a = f(V_{g1k})$ for x-turns = 0.17**

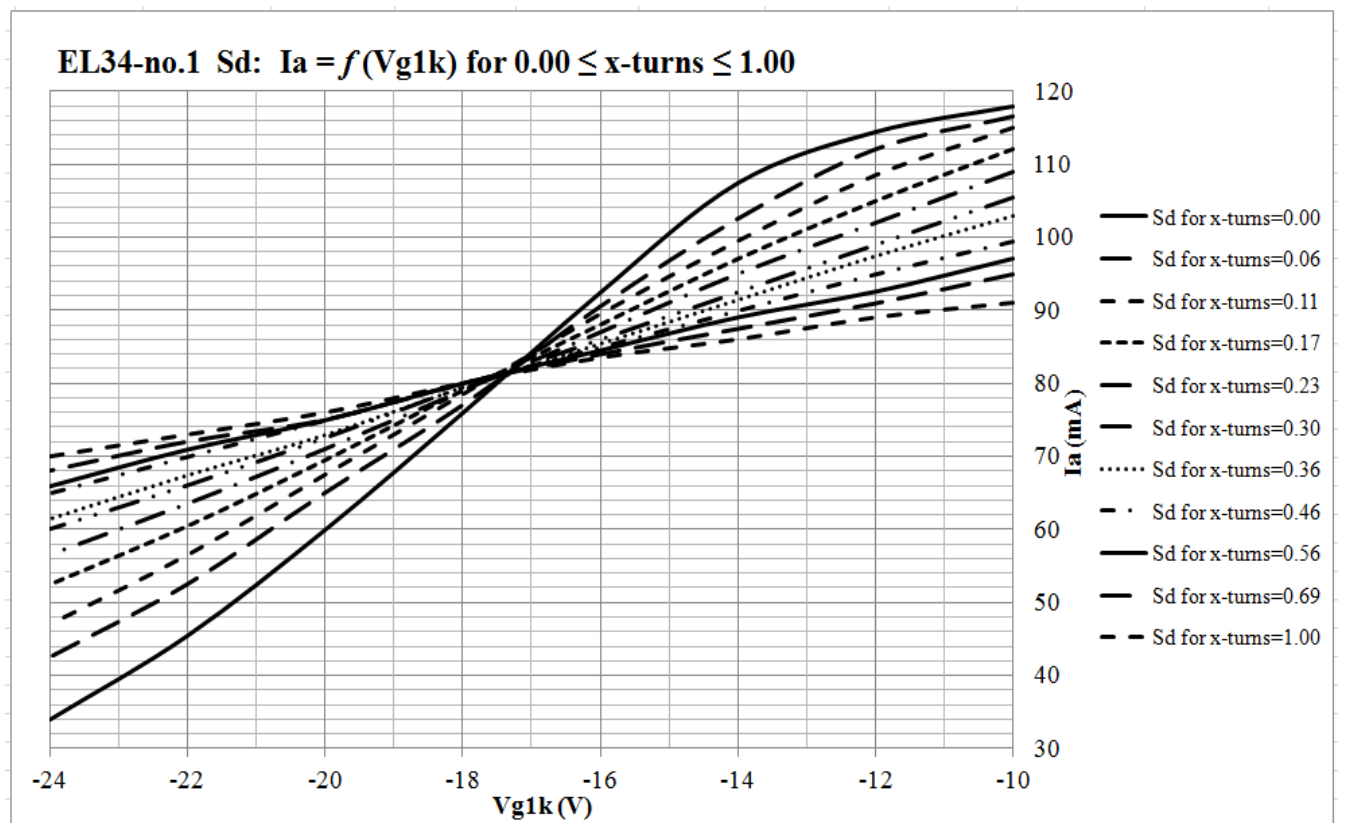
EL34-no.1 Sd: $I_a = f(V_{g1k})$ for x-turns = 0.23**EL34-no.1 Sd: $I_a = f(V_{g1k})$ for x-turns = 0.30**

EL34-no.1 Sd: $I_a = f(V_{g1k})$ for x-turns = 0.36**EL34-no.1 Sd: $I_a = f(V_{g1k})$ for x-turns = 0.46**

EL34-no.1 Sd: $I_a = f(V_{g1k})$ for x-turns = 0.56**EL34-no.1 Sd: $I_a = f(V_{g1k})$ for x-turns = 0.69**

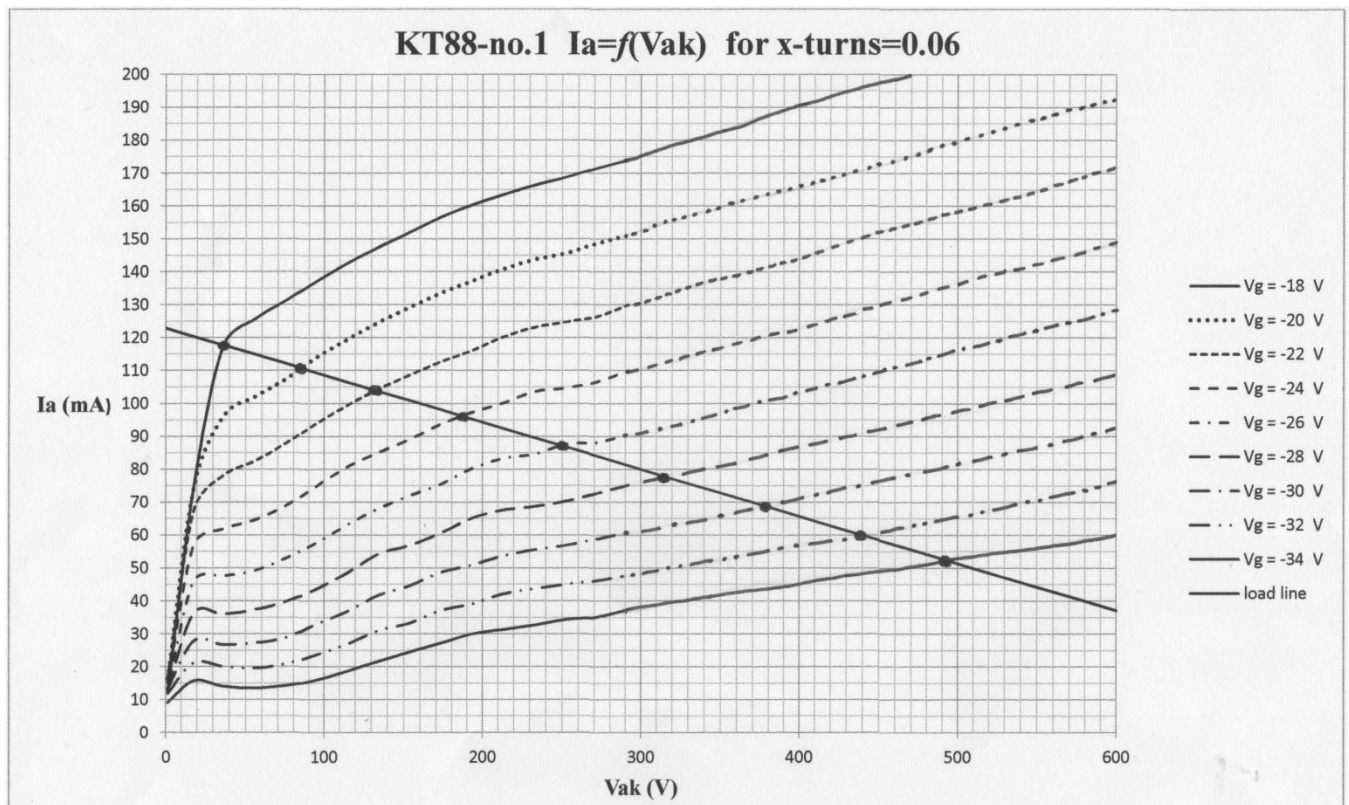
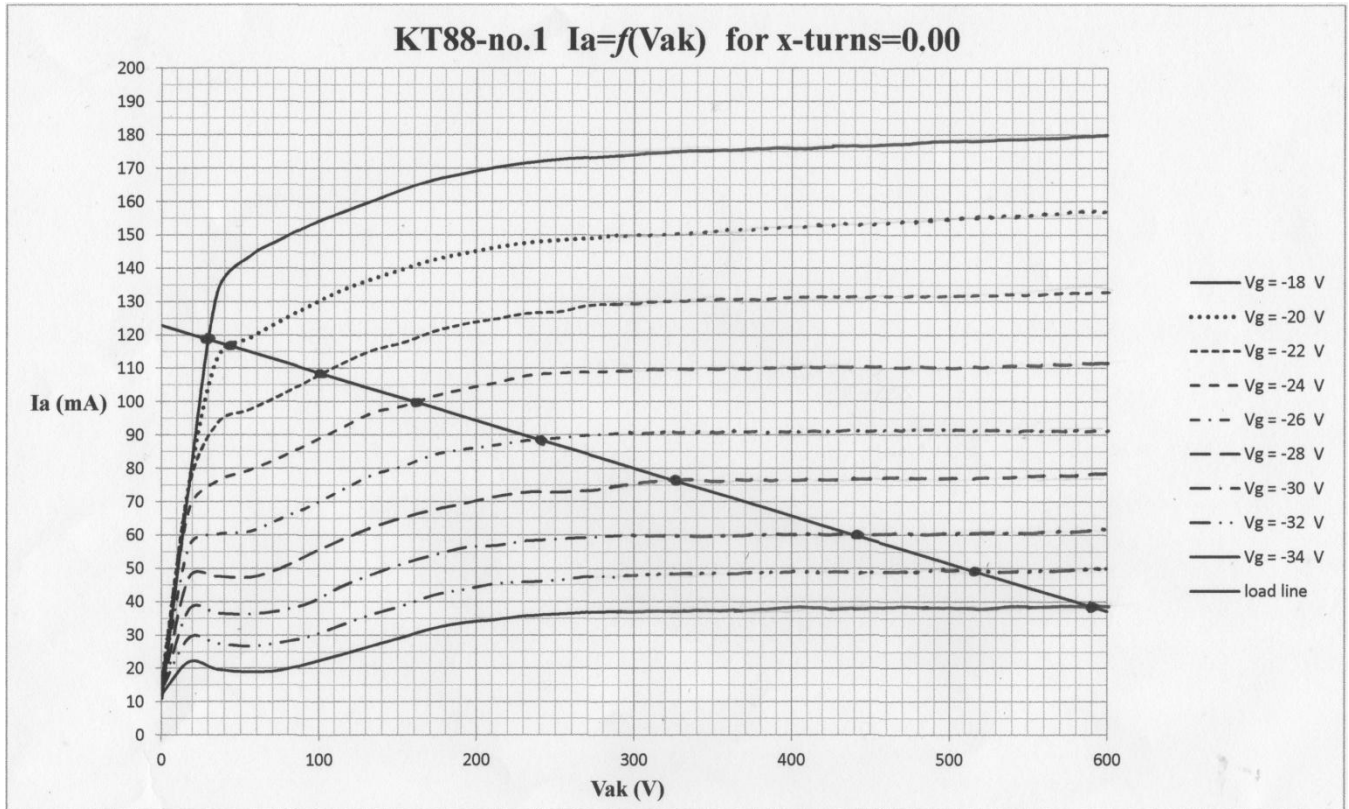


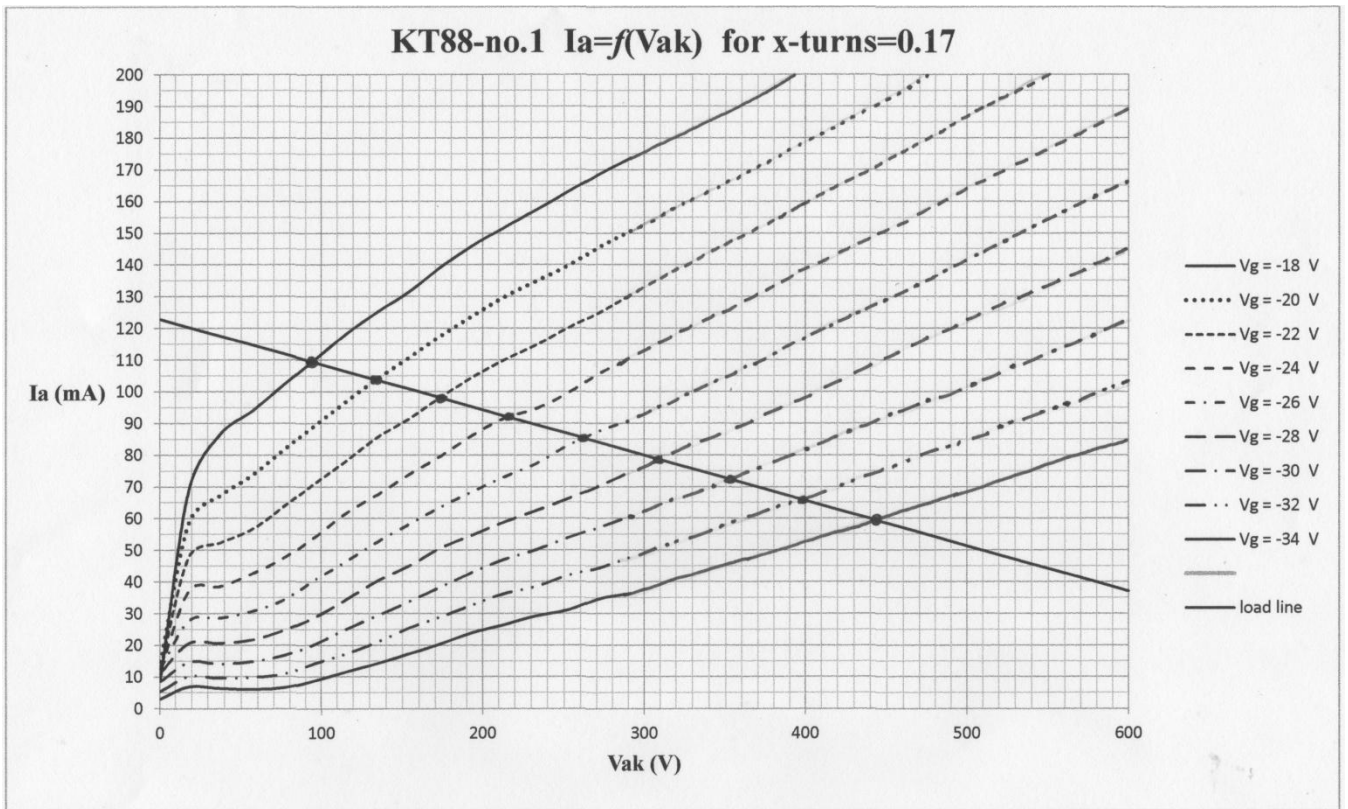
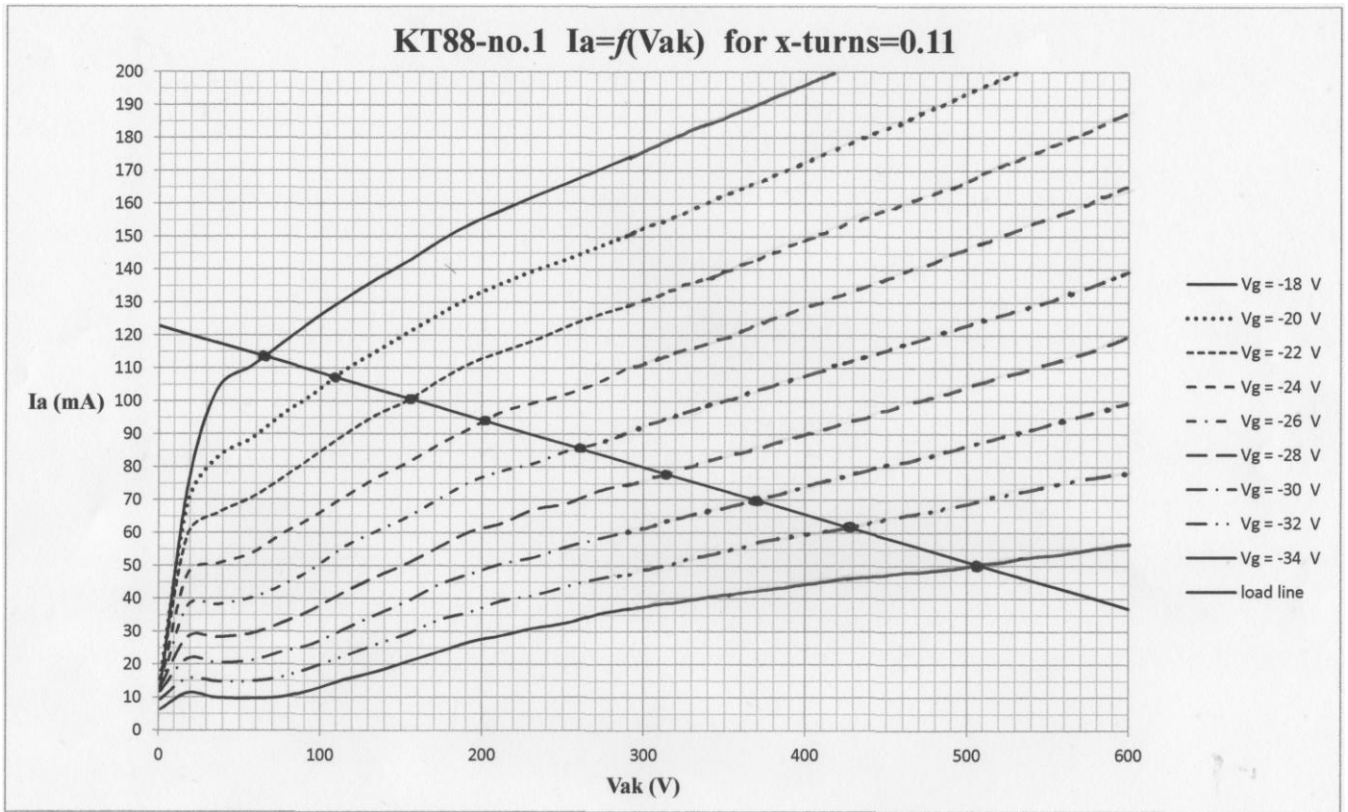
And finally all these S_d together in one transconductance characteristic.

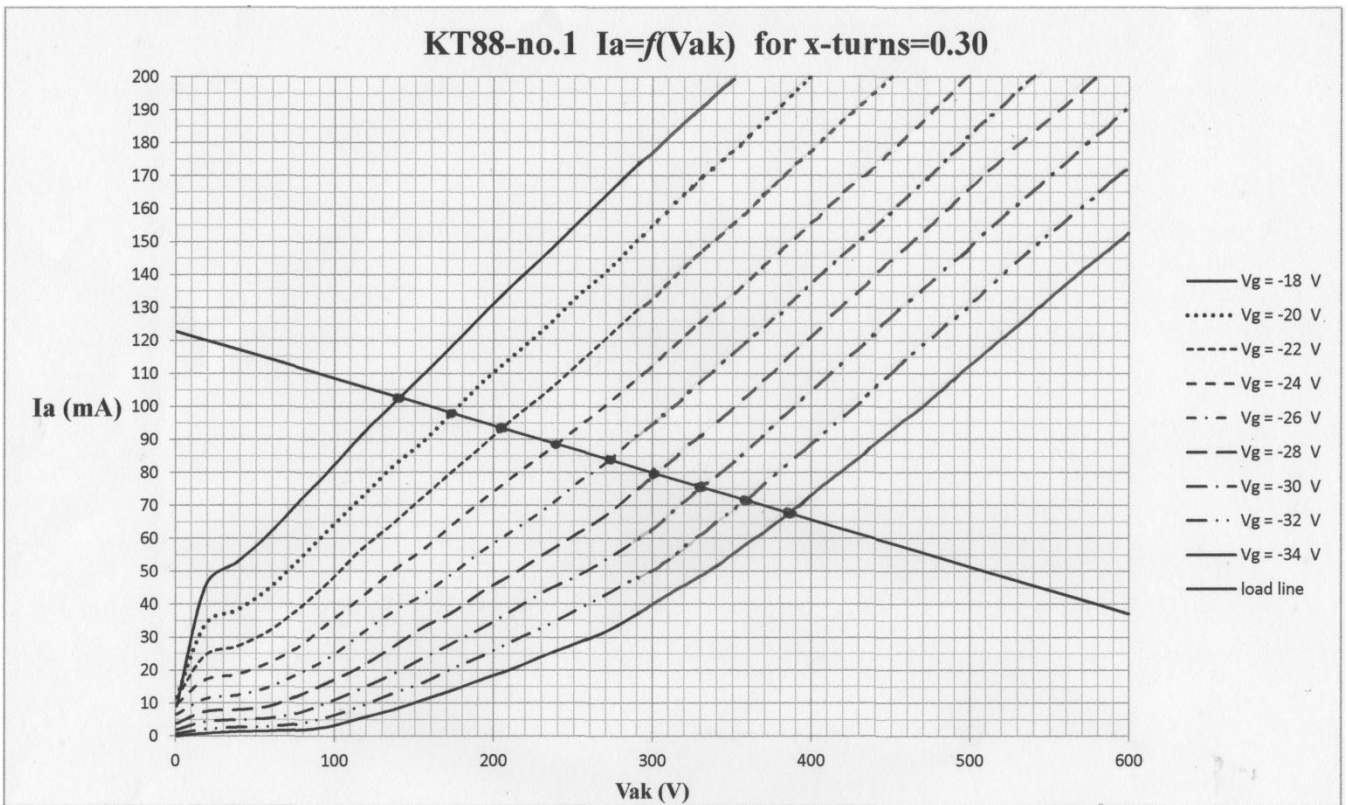
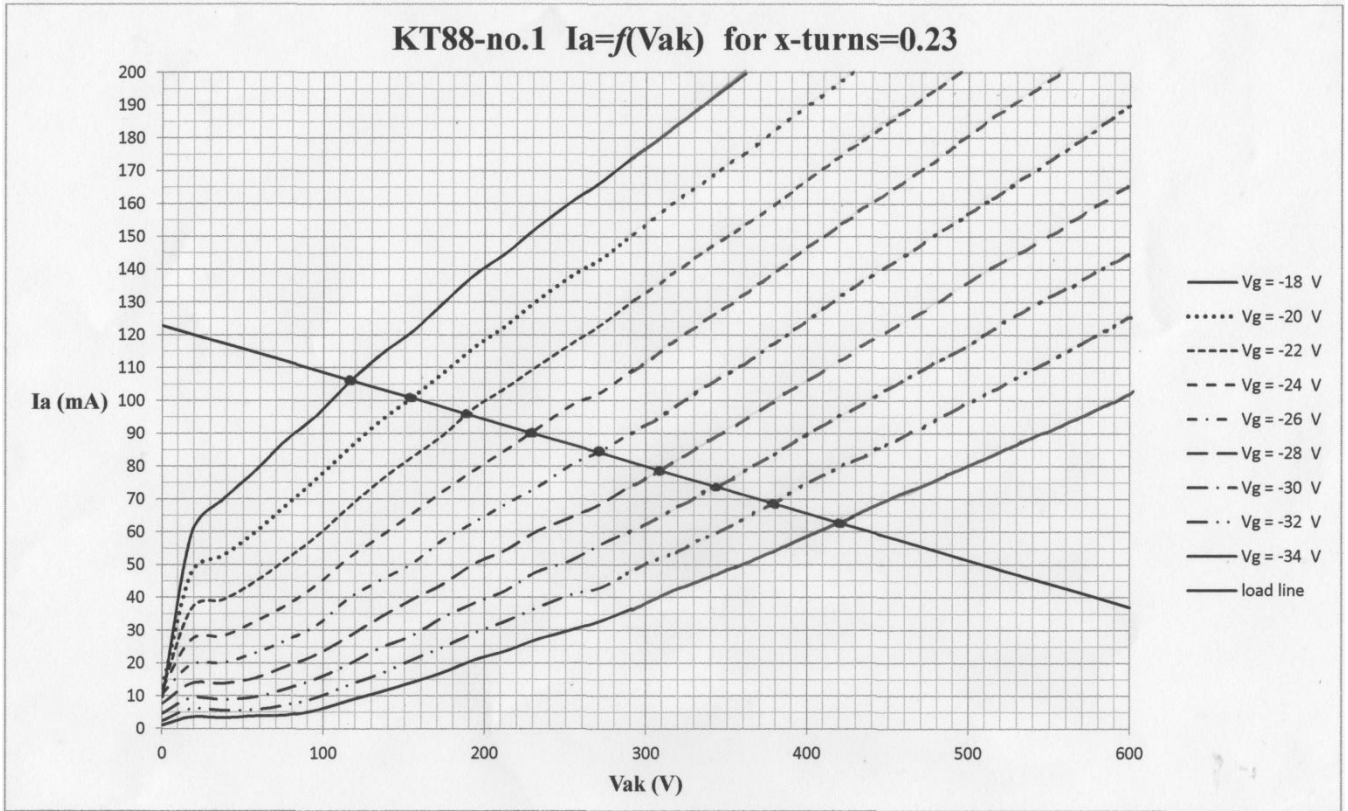


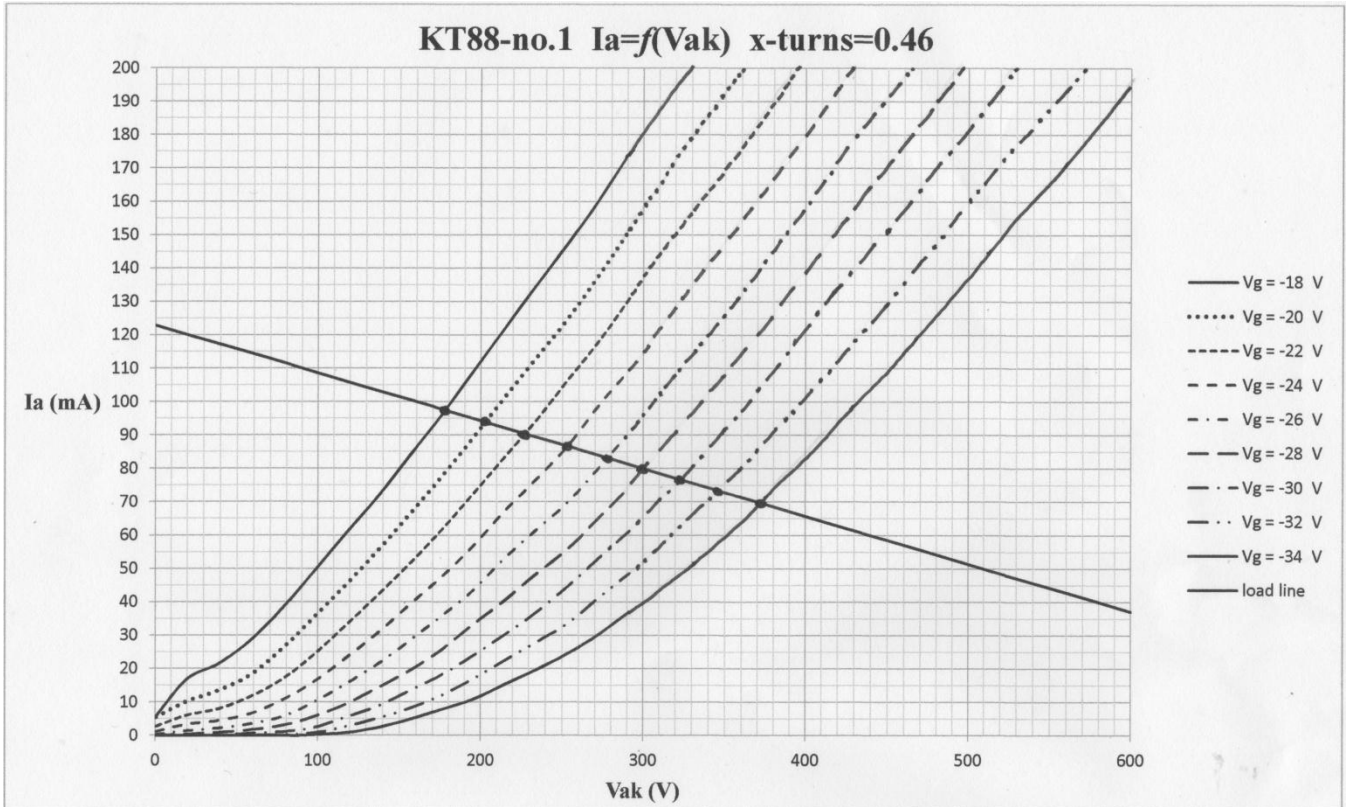
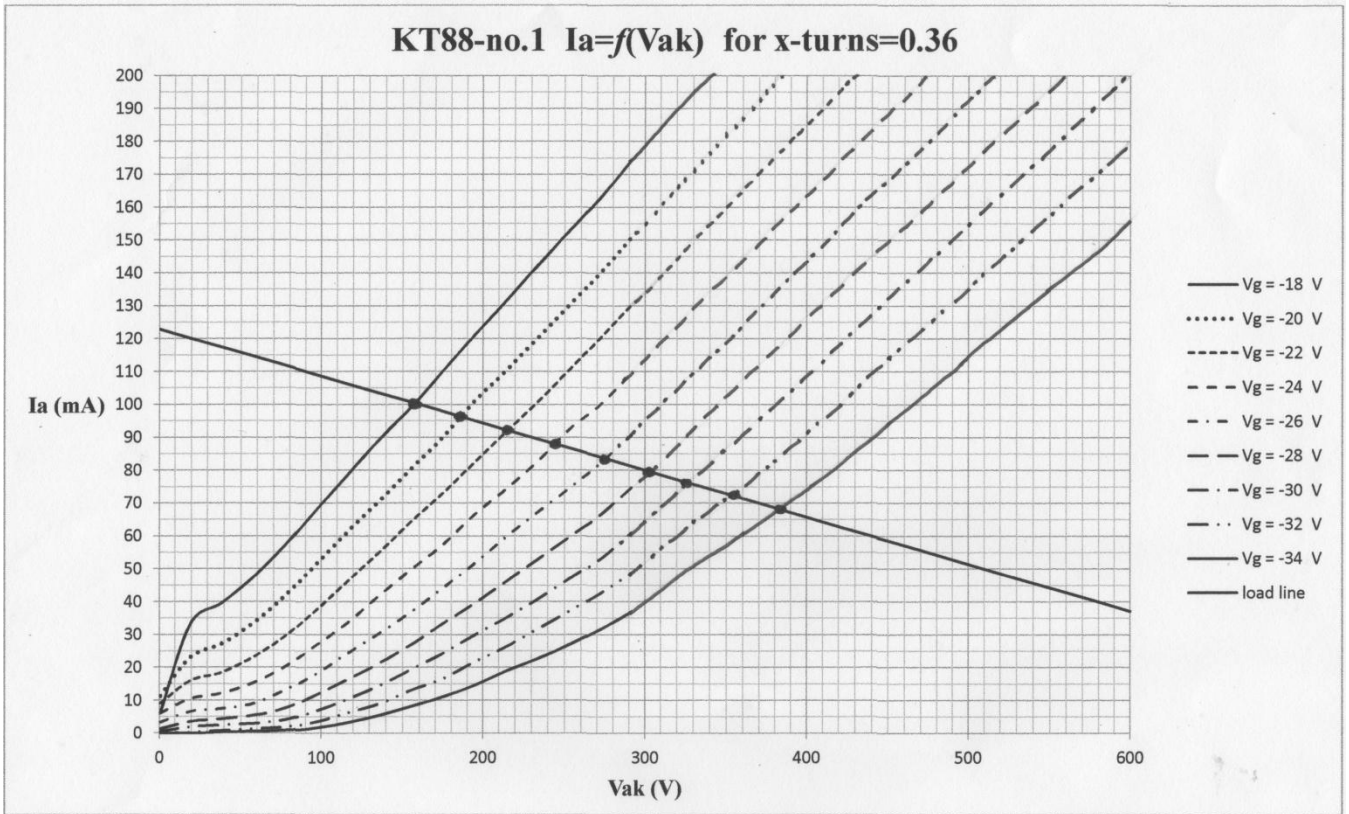
APPENDIX E

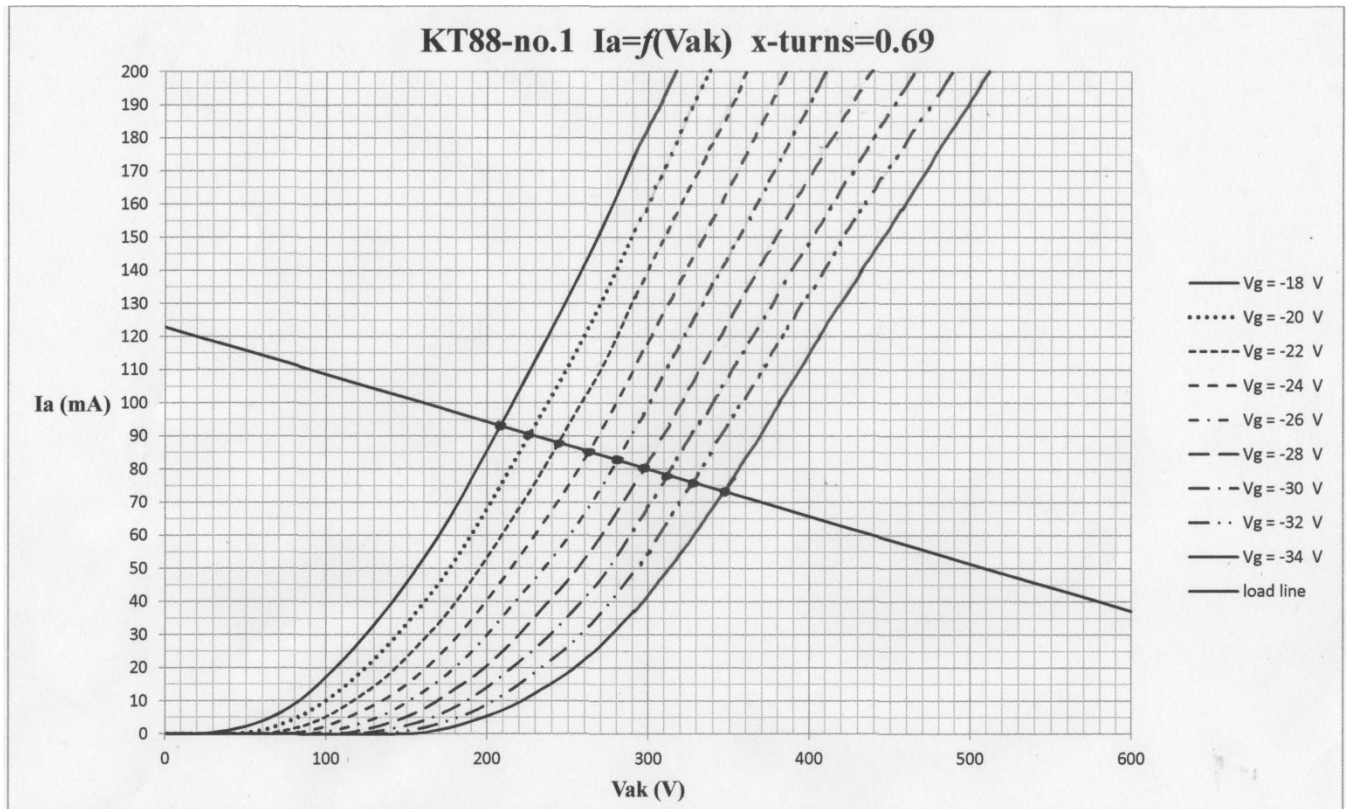
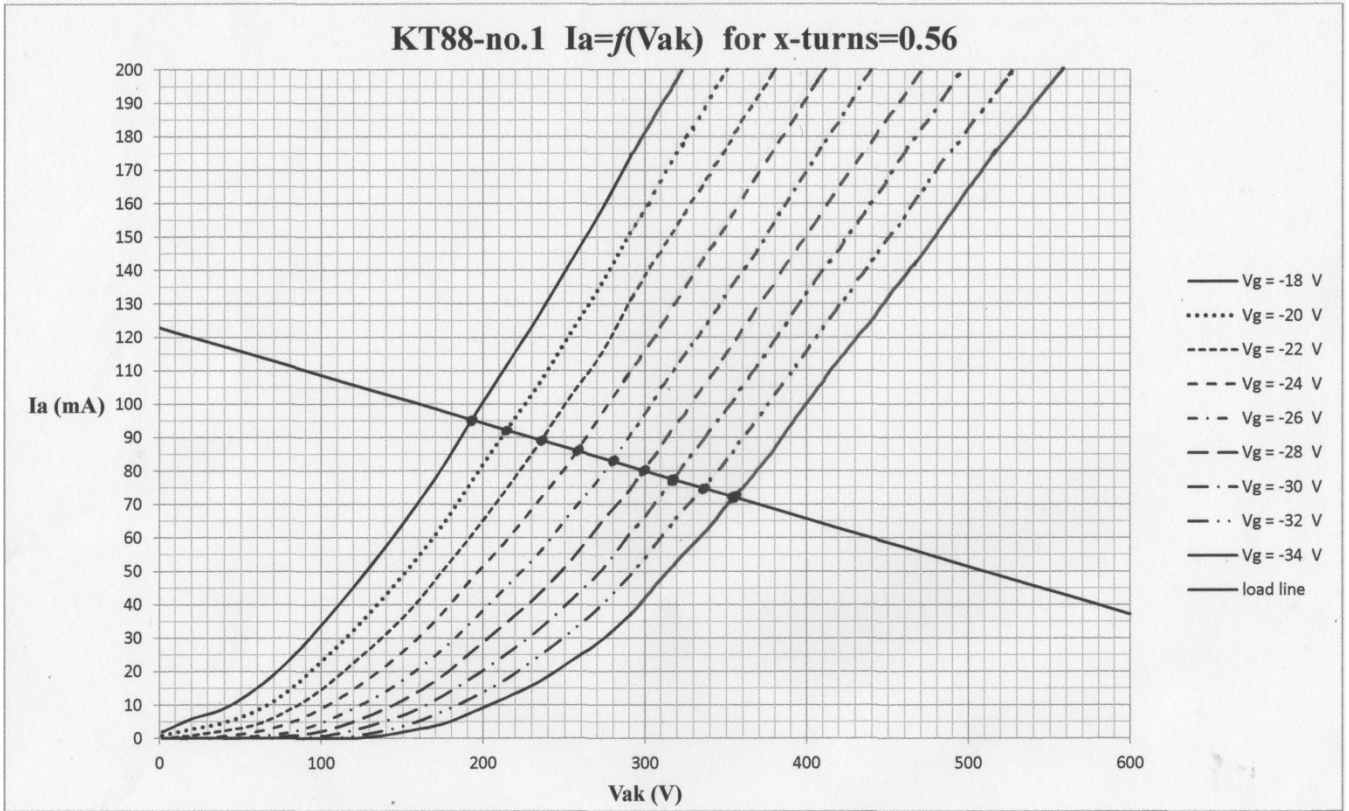
Measured with the μ Tracer and extrapolated anode characteristics of KT88 for several screen grid taps. Load line for KT88 goes through working point $V_{ak,w} = 300\text{V}$, $I_{a,w} = 80\text{mA}$ and $V_{g1k,w} \approx -26.4\text{V}$.





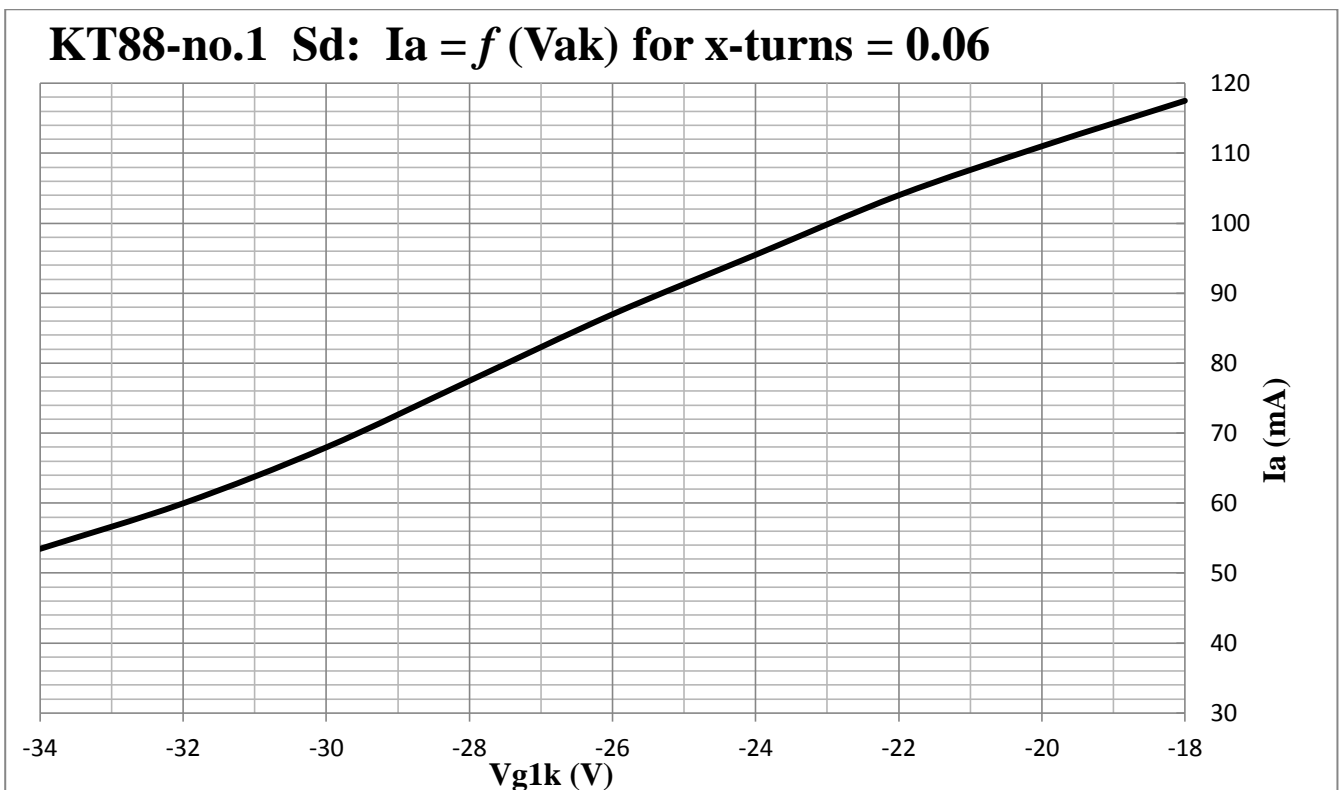
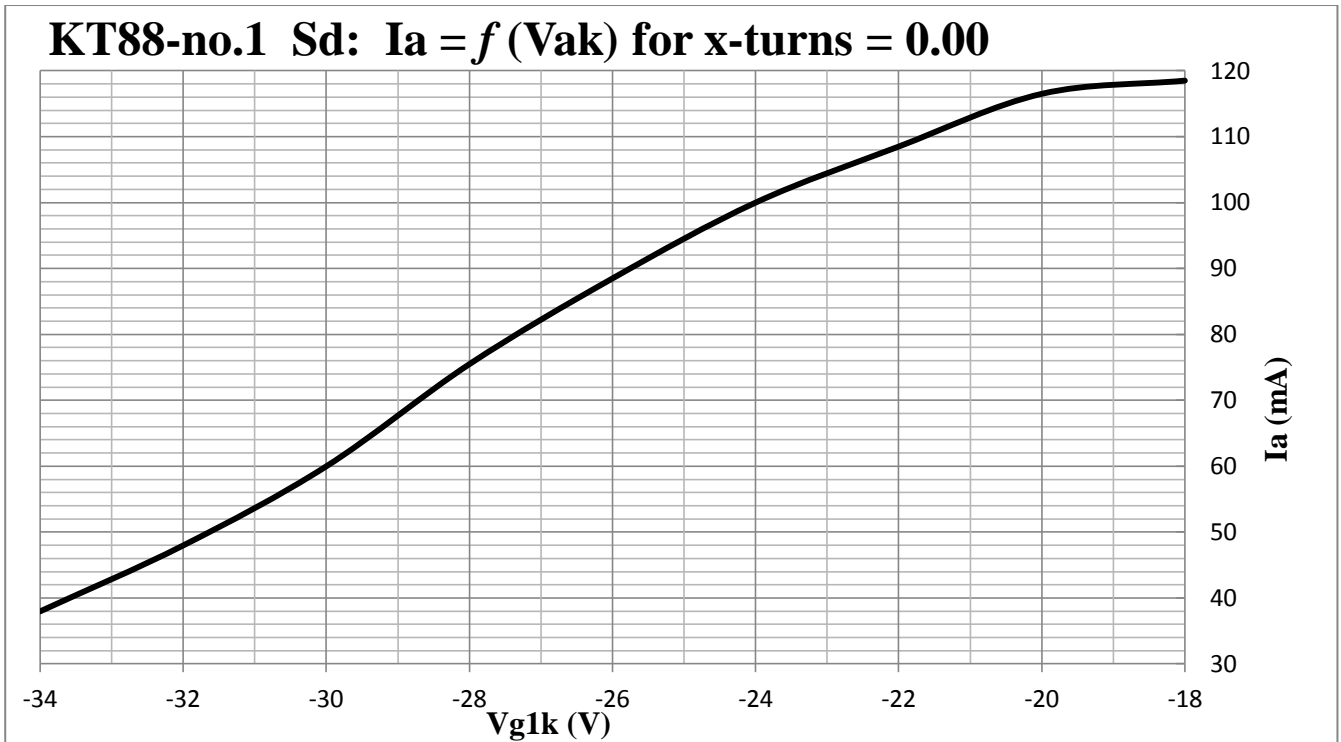


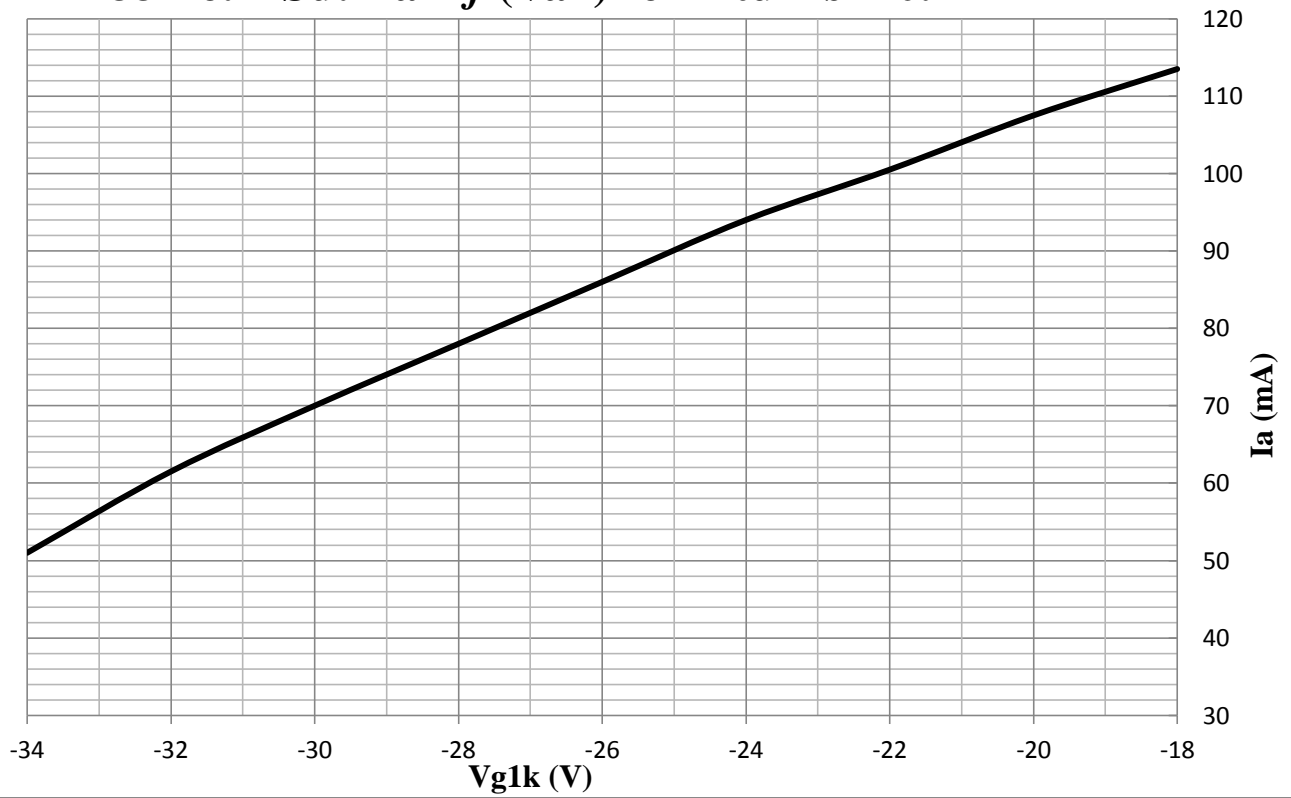
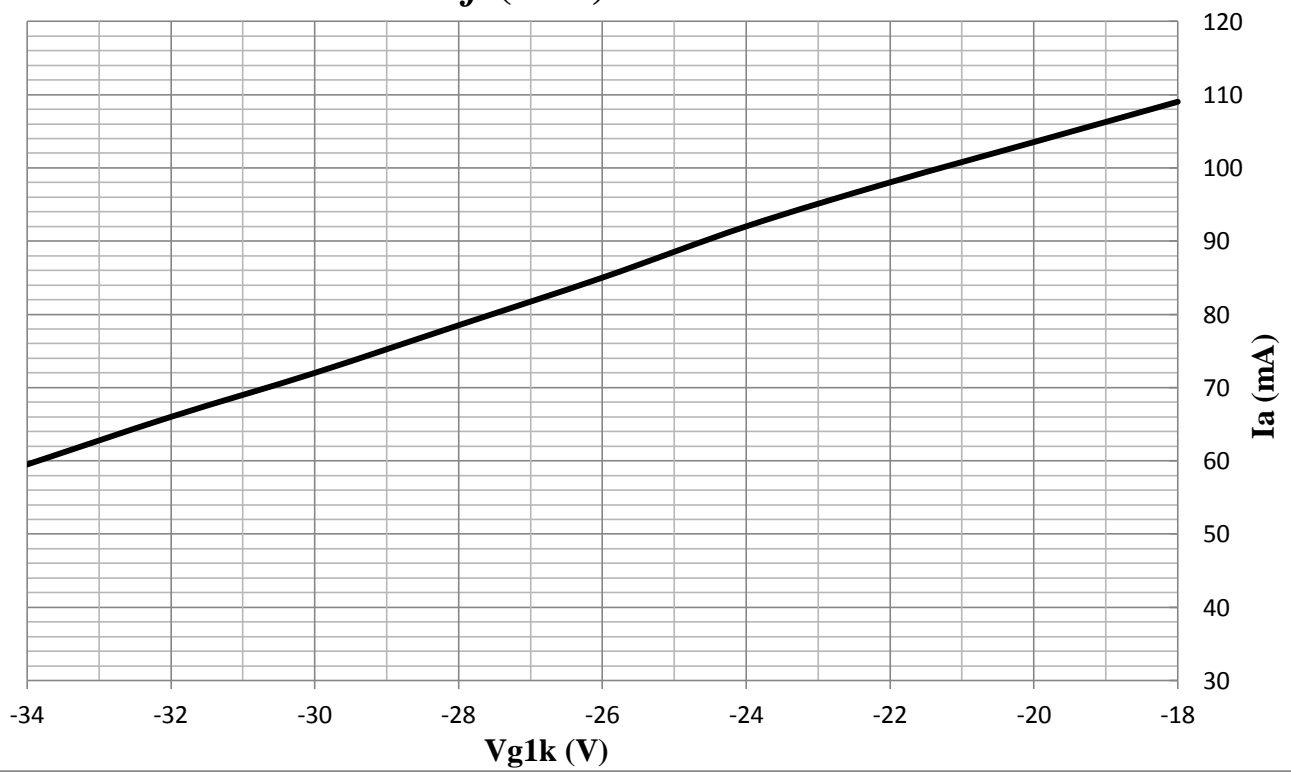


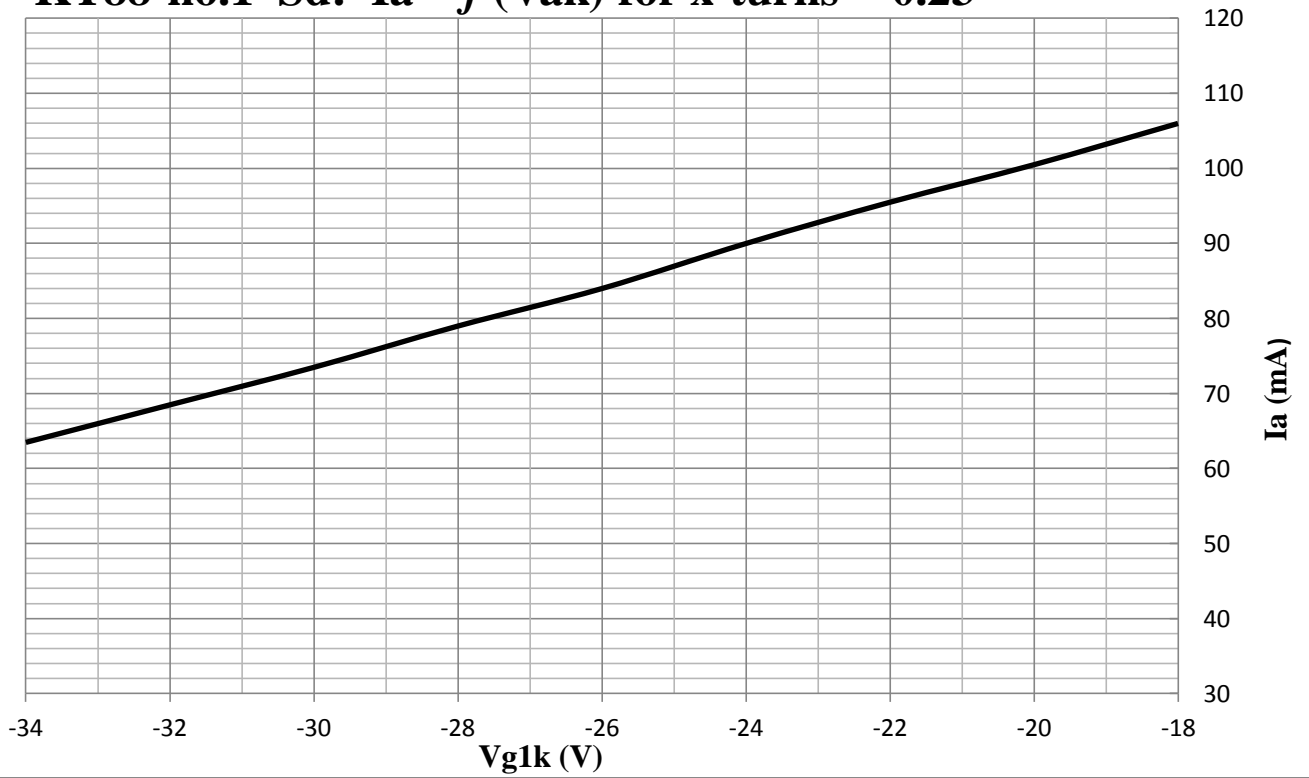
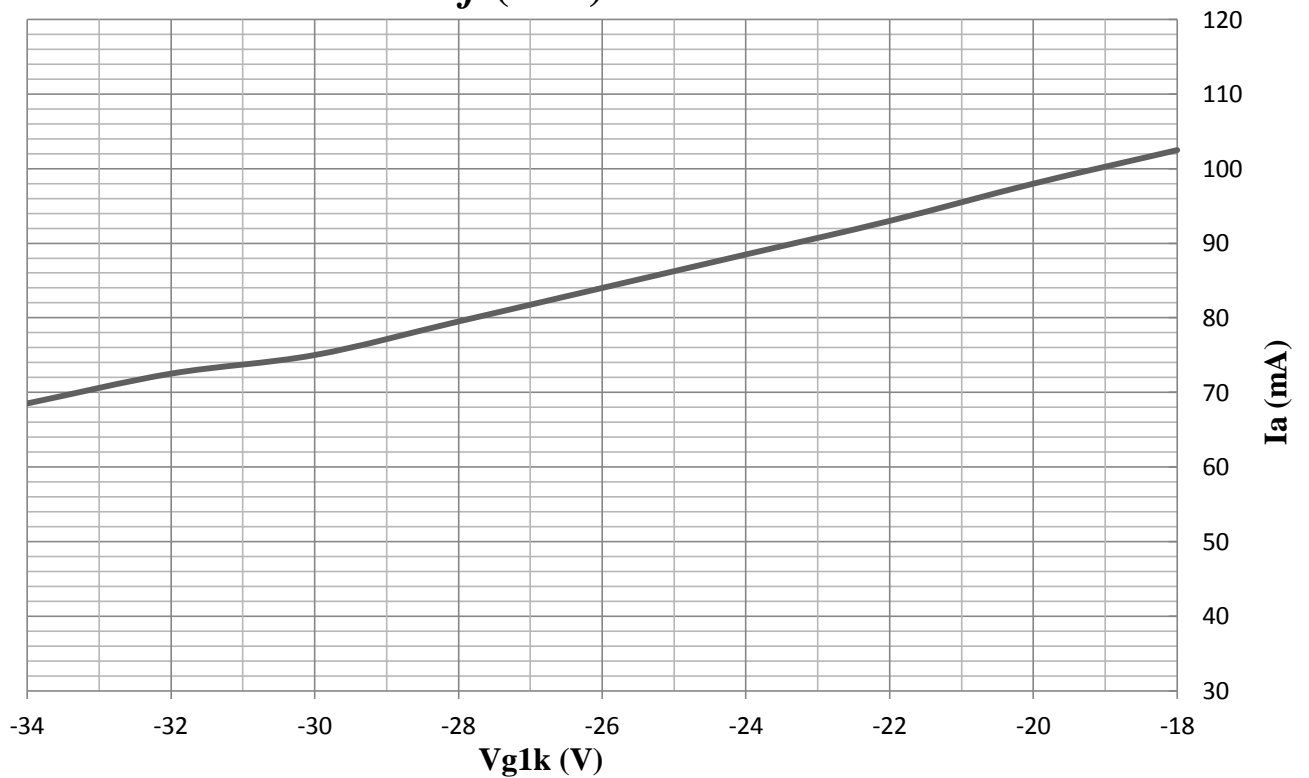


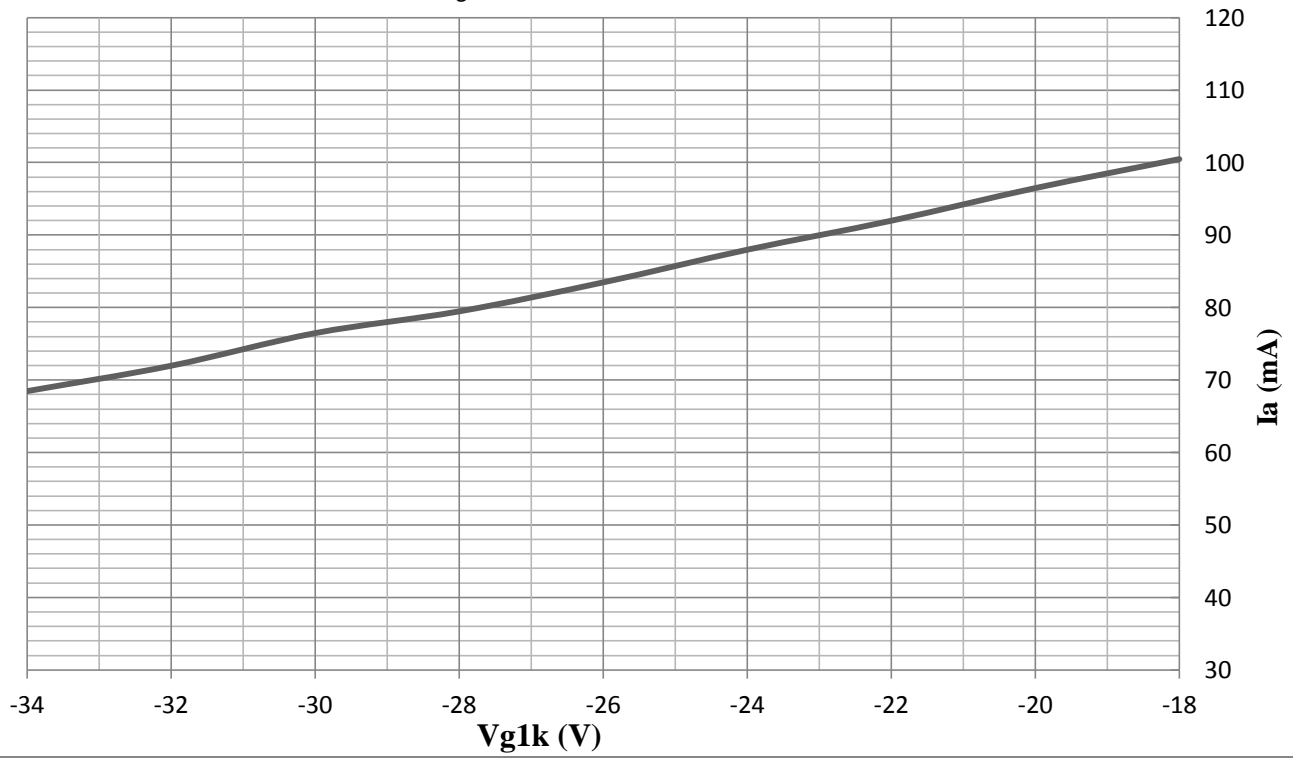
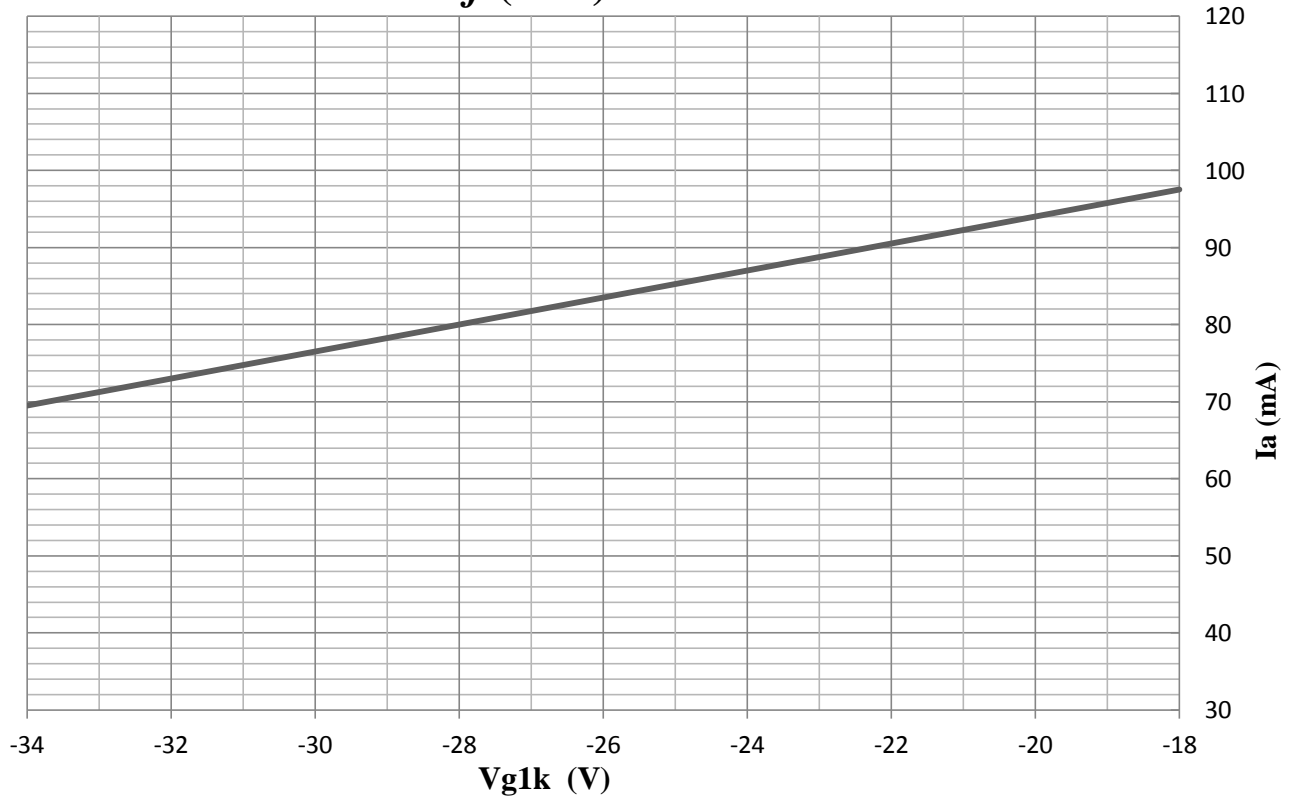
APPENDIX F

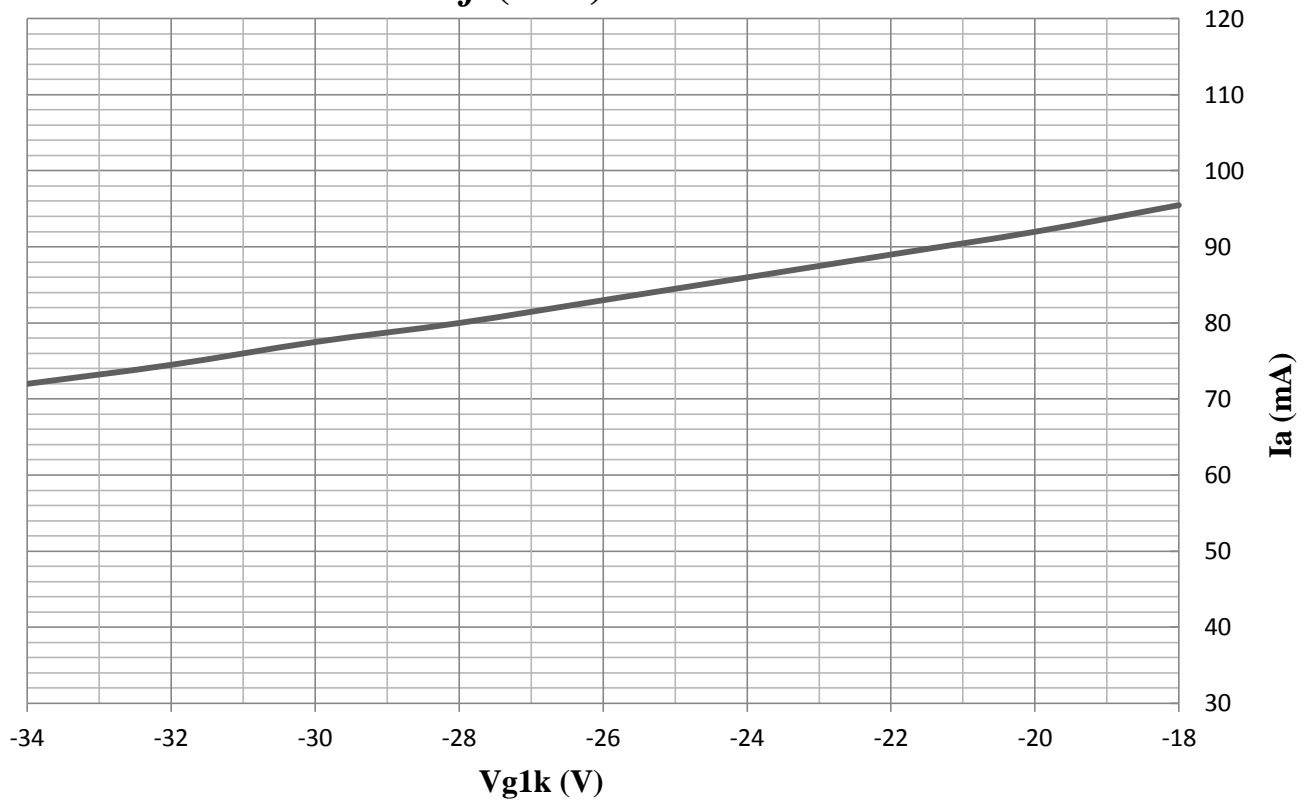
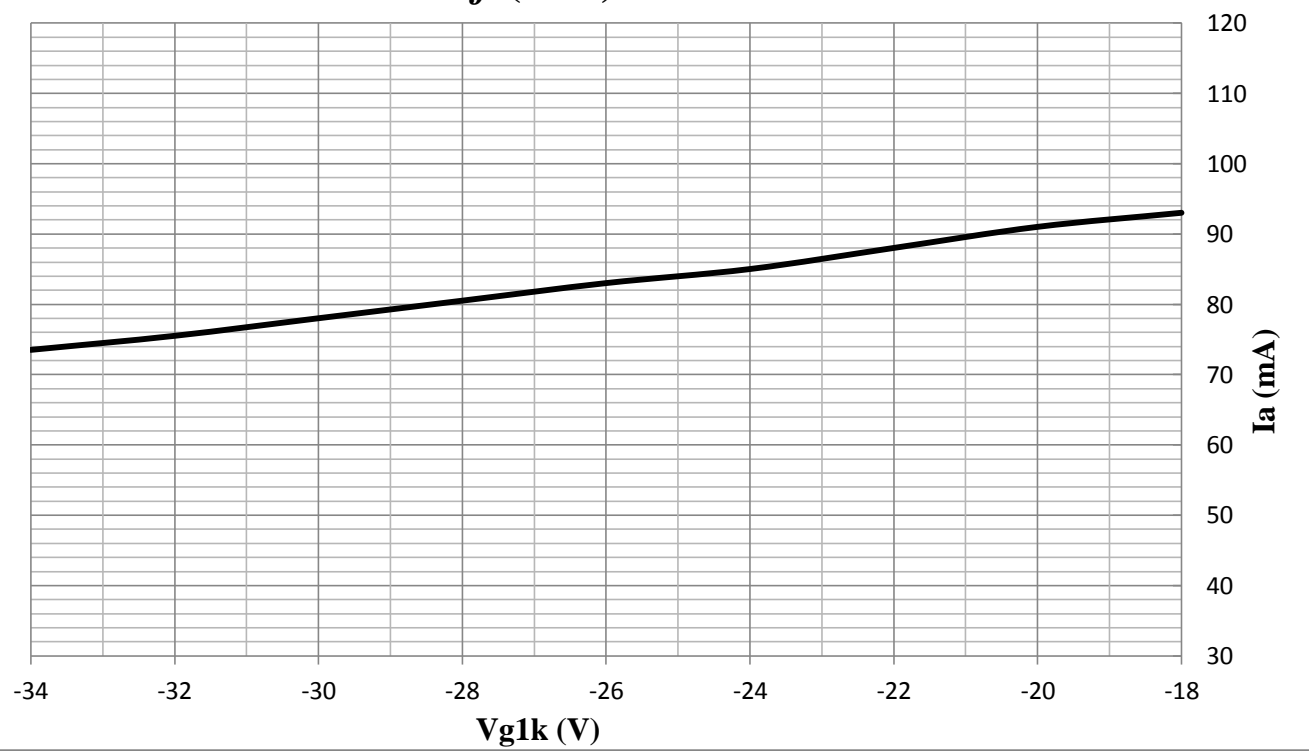
Constructed dynamic transconductance characteristics of KT88 for several screen grid tap.

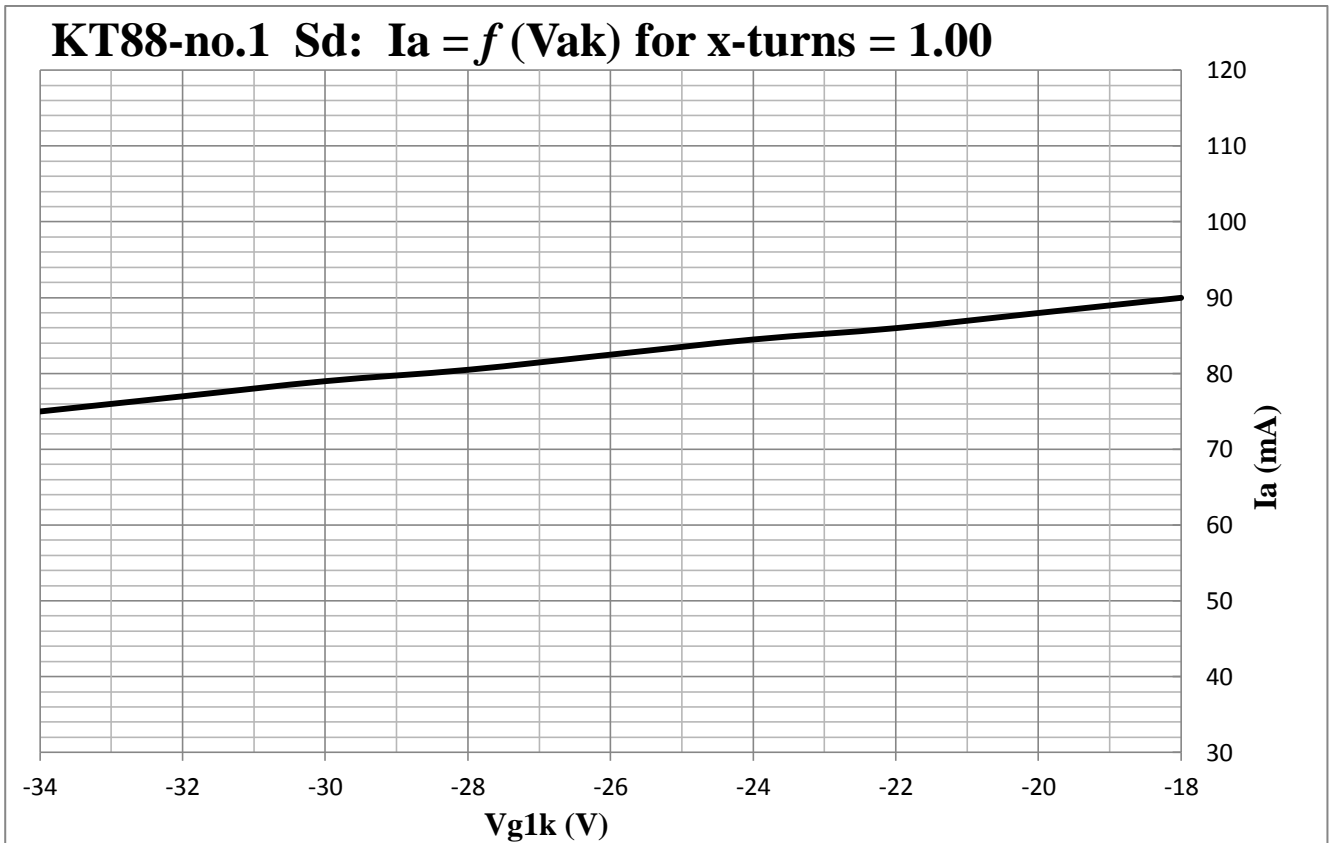


KT88-no.1 Sd: $I_a = f(V_{ak})$ for x-turns = 0.11**KT88-no.1 Sd: $I_a = f(V_{ak})$ for x-turns = 0.17**

KT88-no.1 Sd: $I_a = f(V_{ak})$ for x-turns = 0.23**KT88-no.1 Sd: $I_a = f(V_{ak})$ for x-turns = 0.30**

KT88-no.1 Sd: $I_a = f(V_{ak})$ for x-turns = 0.36**KT88-no.1 Sd: $I_a = f(V_{ak})$ for x-turns = 0.46**

KT88-no.1 Sd: $I_a = f(V_{ak})$ for x-turns = 0.56**KT88-no.1 Sd: $I_a = f(V_{ak})$ for x-turns = 0.69**



And finally all these S_d together in one transconductance characteristic.

